ELSEVIER

Journal of Molecular Structure (Theochem) 400 (1997) 93–117

THEO CHEM

The CO molecule: the role of basis set and correlation treatment in the calculation of molecular properties

Kirk A. Peterson[1,a,b], Thom H. Dunning, Jr.[2,b]

[a]*Department of Chemistry, Washington State University, Richland, WA, USA*
[b]*Environmental Molecular Sciences Laboratory, Pacific Northwest National Laboratory, Richland, WA 99352, USA*

Received 22 January 1997; accepted 29 January 1997

Abstract

Although Hartree–Fock wave functions can provide a semi-quantitative description of the electronic structure of molecules, accurate predictions cannot be made without explicit inclusion of the effects of electron correlation. In correlated calculations, the accuracy of the wave function is determined by two expansions: the many-electron expansion in terms of molecular orbitals that defines the form of the wave function and the basis set used to expand the one-electron molecular orbitals. Thus, to assess the accuracy of a given wave function (correlation method), it is necessary to examine the dependence of a given property on the basis set. In this work, systematic sequences of correlation consistent basis sets ranging in size from double- to sextuple-zeta (cc-pV*n*Z) have been employed together with several commonly used electron correlation methods, e.g., MP*n* (n = 2–4), CCSD, CCSD(T), and MRCI, to calculate the spectroscopic constants and selected molecular properties of the carbon monoxide molecule. The computed spectroscopic constants show excellent convergence toward the complete basis set (CBS) limit, and the *intrinsic* errors of each correlation method have been assessed and compared. The effects of correlating the 1s-like core electrons have also been determined using a sequence of core–valence cc-pCV*n*Z basis sets with the CCSD(T) and ACPF methods. A number of other properties have also been calculated for each correlation method as a function of the correlation consistent basis set: the dipole moment, quadrupole moment, dipole polarizability, and the first and second hyperpolarizabilities. For these calculations, results using the aug-cc-pV*n*Z basis sets are compared with those obtained using basis sets incorporating another complete shell of diffuse functions, d-aug-cc-pV*n*Z. In each case well-behaved convergence toward the CBS limit is observed for each theoretical method. For both the calculated spectroscopic constants and molecular properties, comparisons are made to previous calculations and the available experimental data. © 1997 Elsevier Science B.V.

Keywords: Carbon monoxide; Ab initio; Electronic structure; Spectroscopic constants; Electric moments; Polarizabilities

1. Introduction

Theoretical and computational chemistry have made two invaluable contributions to chemical science. The first is to provide a qualitative framework for interpreting chemical data. Both molecular orbital (MO) and valence bond (VB) theories have filled this role admirably since the late 1920s. Most of our concepts in modern chemistry are based on these theories and it is clear that the MO and VB theories, even with their different viewpoints, provide a fundamentally

[1] E-mail: ka_peterson@pnl.gov
[2] E-mail: th_dunning@pnl.gov

0166-1280/97/$17.00
PII S0166-1280(97)00083-3

correct description of the electronic structure of molecules. With the advent of electronic computers in the late 1950s, a second contribution became possible—the prediction by computation of molecular properties that are too difficult, perhaps even impossible, to determine in the laboratory. Although much progress toward the latter goal was made in the 1960s and 1970s, it was not until the 1980s that computers became sufficiently powerful and the chemistry software sufficiently sophisticated for computational chemistry to realize this contribution. Now, by carefully controlling the errors in the calculations, it is possible to compute the properties of small molecules to an accuracy that rivals that available from all but the most sophisticated experimental studies.

Although molecular orbital wave functions can provide a semi-quantitative description of the electronic structure of molecules, accurate predictions cannot be made without explicit inclusion of the effects of electron correlation. In this case, the accuracy of molecular electronic wave functions is determined by two, inter-related expansions: the many-electron expansion in terms of molecular orbitals that defines the form of the wave function and the basis set used to expand the one-electron molecular orbitals. To assess the accuracy of a given wave function, i.e., a given correlation method, it is necessary to examine the dependence of a given property on the basis set. In the past, the coupling between the correlation method and basis set led to erratic results that limited our understanding of the true errors associated with the chosen correlation method (we shall, in fact, find such examples in the present study of CO). Only by approaching the complete basis set (CBS) limit can the *intrinsic error* of the correlation method be determined, and only when the intrinsic errors of the different correlation methods have been determined can the merits of these methods be unambiguously established.

In the past it was difficult, if not impossible, to obtain reliable estimates of the CBS limits for molecular correlation methods. The basis sets in use did not exhibit regular convergence behavior and the resulting computational requirements were daunting. The family of correlation consistent basis sets are unique among the basis sets [1–6] available today. These sets have been found to exhibit systematic convergence to an apparent CBS limit [7–15]. In addition, these sets are constructed to be as rapidly convergent as possible. As a result, the correlation consistent sets have laid the foundation for systematically estimating CBS limits and understanding the relative accuracies of those correlation methods in widespread use today.

In the present paper, correlation consistent basis sets ranging in size from double- to sextuple-zeta (cc-pV*n*Z), as well as augmented (aug-cc-pV*n*Z, d-aug-cc-pV*n*Z) and core–valence (cc-pCV*n*Z) sets, have been employed together with several commonly used electron correlation methods, e.g., perturbation theory (MP*n*, $n = 2$–4), coupled cluster [CCSD, CCSD(T)], and multireference configuration interaction (icCAS + 1 + 2, icCAS + 1 + 2 + Q), to calculate selected spectroscopic constants and molecular properties of the carbon monoxide molecule. The intrinsic errors of each correlation method, as well as their dependence on basis set, are then assessed and compared.

2. Computational details

The basis sets used throughout the current work are the correlation consistent basis sets of Dunning and co-workers. In the calculation of the potential energy functions (spectroscopic constants), both the cc-pV*n*Z (n = D,T,Q,5,6) and aug-cc-pV*n*Z (n = D,T,Q,5) families of basis sets were used. The cc-pV*n*Z sets range in size from the cc-pVDZ set, [3s2p1d] or 14 contracted functions per atom, to the large cc-pV6Z basis set, [7s6p5d4f3g2h1i] or 140 contracted functions per atom. The aug-cc-pV*n*Z sets were formed from the cc-pV*n*Z basis sets by adding a single set of diffuse functions for each angular symmetry in the standard basis set, with the exponents of the diffuse functions being energy optimized at the CISD (singles and doubles configuration interaction) level for the atomic anions. For investigating the effect of including the 1s-like core electrons in the correlated calculations, additional functions are required to systematically converge the all-electron calculations. For this work the cc-pCV*n*Z (correlation consistent polarized core–valence n–zeta) basis sets, where $n = 2$–5, were used in both valence-only and all-electron calculations. The core–valence basis sets have been developed from the standard cc-pV*n*Z sets by adding functions explicitly optimized for core–core and

core–valence correlation in the atoms. Recent benchmark calculations [16] on the homonuclear diatomics of the first row have demonstrated that these sets also systematically converge toward the complete basis set limits for all-electron calculations in much the same way that the standard valence sets converge toward the valence-only CBS limits.

In the calculation of molecular properties, the basis set requirements can be very different than what is observed for spectroscopic constants. In particular, for properties such as dipole polarizabilities or, especially, hyperpolarizabilities, extra diffuse functions are required for an accurate determination of the property (cf., Ref. [4]). Two additional sequences of basis sets have been considered for the calculation of molecular properties: the aug-cc-pVnZ (n = D, T, Q, 5) basis set described above, as well as these sets augmented by an additional shell of diffuse functions, d-aug-cc-pVnZ (n = D, T, Q). These doubly augmented sets have previously been shown [4] to significantly improve the description of hyperpolarizabilities in calculations on the rare gas atoms.

In all calculations only the pure spherical harmonic components of the polarization functions have been used.

One of the most important features of using the hierarchial sequence of correlation consistent basis sets is their systematic convergence toward the apparent complete basis set (CBS) limit. This is in part due to the systematic convergence of the atomic correlation energies for which the correlation consistent basis sets were developed. As has now been shown in a large number of benchmark calculations [7–15], this behavior is also observed for molecular total energies, energy differences, and some spectroscopic constants. Often the basis set convergence can be modeled by a simple exponential function:

$$A(n) = A_\infty + Be^{-Cn}$$

to obtain estimates of the complete basis set limits A_∞; other extrapolation procedures have been explored by Wilson and Dunning [17]. In the present work estimated CBS limits for the dissociation energies have been obtained as differences between extrapolated total energies, however it has been noted previously that sometimes extrapolation of the dissociation energies themselves results in better overall fits.

After estimating the CBS limit for each correlation method, the remaining differences with respect to experiment are a measure of the errors intrinsic to that method. As has been demonstrated previously for the N_2 molecule [15], comparing the inherent accuracy of different correlation methods is only unambiguous near the CBS limit, where coupling between the one-particle and n-particle basis sets approaches zero. In the present work, CBS limits obtained by exponential extrapolation have been estimated whenever a property exhibited suitably smooth convergence.

Correlated wave functions based on both a single configuration and a multiconfigurational reference wave function have been employed in the present work. The single reference methods were based on self-consistent field (SCF) orbitals and included second, third, and fourth order Møller–Plesset perturbation theory [18] (MP2, MP3, and MP4, respectively) as well as single and doubles coupled cluster (CCSD) and CCSD with the addition of a perturbative estimate of triple excitations, CCSD(T) [19] In the multireference calculations, the orbitals were taken from full valence ($1-6\sigma$, $1-2\pi$) complete active space self-consistent field (CASSCF) calculations [20,21] in which the 1σ and 2σ core orbitals were constrained to be doubly occupied.

In the multireference calculations, steps had to be taken to prevent mixing between the $1-2\sigma$ orbitals (1s-like) and the $3-4\sigma$ orbitals (2s-like). While the CASSCF wave function is invariant with respect to unitary transformations among these orbitals, the subsequent MRCI calculations are not since the $1-2\sigma$ orbitals are not correlated. Poor resolution of frozen core orbitals can artificially raise MRCI energies and degrade the predicted spectroscopic constants. As in our previous work [8,9,15], we resolved the core orbitals by carrying out a two-step CASSCF procedure at each distance. In the first step, the $1-4\sigma$ orbitals were constrained to be doubly occupied; in this way they can be uniquely defined as eigenfunctions of an effective Fock matrix [22]. The $1-2\sigma$ orbitals from this first calculation were then frozen and used in a second CASSCF with the full valence active space described above. In each case these latter CASSCF orbitals were then used in subsequent CAS-reference singles and doubles internally contracted MRCI calculations [23,24] (icMRCI or icCAS + 1 + 2), where the doubly external configurations were internally contracted. In

the present work, resolving the core orbitals increased the icCAS + 1 + 2 D_e values by about 0.2 kcal mol^{-1} and decreased the r_e values by about 0.001 Å. Estimates of higher excitations have been obtained by application of the multireference analog of the Davidson correction [25–27], icMRCI + Q (icCAS + 1 + 2 + Q). Unless otherwise noted, the frozen core approximation was used throughout.

Since an assessment of the effects of core correlation involves comparing calculations with different numbers of correlated electrons, the use of size extensive methods is expected to produce more accurate results. This condition is satisfied by the CCSD(T) wave functions and this method has been previously shown to yield excellent results for predicting the effects of core correlation [16,28–31]. Since the icMRCI + Q method is only approximately size extensive, the multireference internally contracted averaged coupled pair functional method [32,33], icACPF, has also been used for these calculations.

For each species, potential energy functions were calculated by fitting nine computed energies that covered a range of $-0.4a_0 \leq \Delta r \leq +0.7a_0$ to seventh- or eighth-order polynomials in $\Delta r = r - r_e$. Spectroscopic constants were then determined from the fitted polynomial coefficients by the usual Dunham analysis [34]. In the calculation of dissociation energies, the dissociated limits were computed in two ways. For the Hartree–Fock-based methods, these were obtained from calculations on the isolated atoms. For the perturbation theory methods, ROHF-MPn wave functions [35] were employed as implemented in the ACES-II program package.[3] Coupled cluster calculations on the atoms were carried out with the partially spin-restricted RCCSD method of Knowles and Werner [37,38] as implemented in the MOLPRO program. In the RCCSD atomic calculations, the symmetry equivalencing was consistent with dissociating the molecular system, i.e., the orbitals were taken from state averaged SCF calculations that provided symmetry equivalencing of the P_x and P_y components. In the icMRCI and icACPF calculations, the dissociated limits were obtained in supermolecule calculations with $r = 50a_0$. With the exception of the open-shell MPn work, all calculations in this work were carried out with the MOLPRO suite of ab initio programs.[4]

An additional aspect that must be considering when comparing the present ab initio dissociation energies with the experimental values is that the former do not include spin–orbit effects, while the latter are referenced to the spin–orbit ground states of the atoms. Hence, as in our previous work [7–9], we have removed these relativistic effects from the experimental value using the atomic energy level data of Moore [40], yielding an "experimental" D_e that can be directly compared with our ab initio values. In the present case, these corrections amount to adding 0.083 kcal mol^{-1} from carbon atom and 0.216 kcal mol^{-1} from oxygen to the experimental D_e [41] of 259.26 ± 0.09 kcal mol^{-1} (corrected for zero-point vibrations using the spectroscopic constants of Ref. [42]) to yield a D_e of 259.56 ± 0.09 kcal mol^{-1}. Of course, this assumes that the atomic products are in their ground spin–orbit states in the determination of D_e. This assumption, however, has also been used to derive the heat of formation of C(g) in the current supplement to the JANAF tables [43].

The following molecular electric properties of CO have also been calculated in the present work: the dipole moment μ_z, quadrupole moment Θ_{zz}, dipole polarizabilities α_{zz} and α_{xx}, first hyperpolarizabilities β_{zzz} and β_{xxz}, and second hyperpolarizabilities γ_{zzzz}, γ_{xxxx}, and γ_{xxzz}. In general, these were determined as derivatives of the total energy with respect to either dipole (μ, α, β, and γ) or quadrupole (Θ) electric fields. Furthermore, the quadrupole moment was computed relative to the center of mass of the molecule. The dipole and quadrupole moments were also calculated as expectation values for the icMRCI wave functions. The difference between the dipole moments

[3] ACES-II is a computational chemistry package especially designed for CC and MBPT energy and gradient calculations. Elements of this package are: the SCF, integral transformation, correlation energy, and gradient programs written by J.F. Stanton, J. Gauss, J.D. Watts, W.J. Lauderdale, and R.J. Bartlett; the VMOL integral and VPROPS property integral programs written by P.R. Taylor and J. Almlöf; a modified version of the integral derivative program ABACUS written by T. Helgaker, H.J. Jensen, P. Jørensen, J. Olsen, and P.R. Taylor; and the geometry optimization and vibrational analysis package written by J.F. Stanton and D.E. Bernholdt.

[4] MOLPRO is a package of ab initio programs written by H.-J. Werner and P.J. Knowles with contributions from J. Almlöf, R.D. Amos, M.J.O. Deegan, S.T. Elbert, C. Hampel, W. Meyer, K.A. Peterson, R.M. Pitzer, A.J. Stone, P.R. Taylor, and R. Lindh.

computed as an energy derivative and as an expectation value was 0.015 D near the complete basis set limit (aug-cc-pV5Z), where the energy derivative value was smaller in magnitude and closer to experiment. This is very similar to the result obtained in the recent work of Langhoff and Bauschlicher [44] and somewhat larger than that of Ernzerhof et al. [45]. The analogous difference between the quadrupole moments was calculated to be 0.017 a.u., and again the energy derivative value was closer to experiment. In the remainder of this work, only properties evaluated as energy derivatives will be presented. The derivatives of the energy with respect to an applied field were carried out via the usual finite difference approach. The finite difference formulas given by Bartlett and Purvis [46] were used for μ, Θ, α, β_{xxz}, and γ_{xxzz}; higher order formulas were used for the diagonal terms of β and γ (5th order and 6th order, respectively). Since the evaluation of β and γ require third and fourth derivatives of the energy with respect to a field, care was taken to avoid numerical imprecision in the resulting tensor components. Hence, all energies were converged to near-machine precision and several convergence tests were made to assess the effects on the resulting β and γ components. In nearly all cases the base field strength value was 0.004 a.u., which was chosen after several test calculations to maximize the accuracy of the resulting properties and minimize numerical inaccuracies.

While most of the properties outlined above were computed only at the experimental equilibrium distance of $2.1322a_0$ [42], the effects of vibrational motion were investigated for the CCSD(T) dipole moments, quadrupole moments, and dipole polarizabilities. The entire aug-cc-pVnZ basis set series (n = 2–5) was employed for the dipole moment calculations, while only the aug-cc-pV5Z basis set was investigated for the quadrupole moment and polarizabilities. In each case, both μ and α were computed at the same geometries as in the potential energy function calculations and fit to polynomials of 4th order in Δr. The dipole field strength for these calculations was 0.002 a.u. Rotationless vibrational matrix elements were then calculated by using vibrational wave functions obtained from an accurate RKR potential function [47] by numerical solution of the Schrödinger equation using Cooley's method [48]. The effects of zero-point vibrations on the quadrupole moment and polarizabilities obtained in this way were applied to the experimental $v=0$ quantities to obtain estimates of the equilibrium values for comparison with our calculations at fixed $r = r_{expt}$. Unlike the other properties reported here, the equilibrium dipole moment of CO is known accurately from experiment [49,50].

3. Results and discussion

3.1. Spectroscopic constants

3.1.1. Standard sets

Consider first the spectroscopic constants of CO obtained with the standard cc-pVnZ basis sets. These results are summarized in Tables 1 and 2. In regard to the SCF methods (HF, CASSCF), two points are immediately obvious. Firstly, the HF approximation alone yields extremely poor results for the CO molecule: D_e is underestimated by nearly 75 kcal mol^{-1}, r_e is too short by 0.026 Å, and the harmonic frequency is too large by more than 250 cm^{-1}. Secondly, most of the error in these quantities is removed when the CASSCF method is utilized. From the CASSCF calculations the corresponding errors are: -7.2 kcal mol^{-1} (D_e), 0.0043 Å (r_e), and -0.7 cm^{-1} (ω_e). In regards to the one-particle basis set, both methods have very similar convergence behavior and are essentially converged to their respective CBS limits with the cc-pVQZ basis set. Our calculated SCF/cc-pV6Z total energy at the experimental bond distance of $2.1322a_0$ of $-112.790841E_h$ is in good agreement with the numerical Hartree–Fock result of Sundholm et al., $-112.79095E_h$, obtained at $r=2.132a_0$. Use of the exponential extrapolation discussed above on the cc-pVTZ through cc-pV6Z SCF energies (at $r=2.1322a_0$) yields an estimated CBS limit at the experimental equilibrium separation of $-112.79097E_h$, in essentially exact agreement with the numerical HF value.

The dependence of D_e, r_e, and ω_e on the basis set is plotted in Figs. 1–3 for the three different correlation approaches studied here: the internally contracted multireference configuration interaction (icCAS + 1 + 2), perturbation theory (MP2, MP3, MP4), and coupled cluster [CCSD, CCSD(T)] methods. These results are reminiscent of our earlier work on the

Table 1
Calculated spectroscopic constants of CO compared with experiment. Methods based on single configuration wave functions

Method	Basis set	E_e (a.u.)	r_e (Å)	ω_e (cm^{-1})	$\omega_e x_e$ (cm^{-1})	α_e (cm^{-1})	D_e (kcal mol^{-1})
Experimental [a]			1.1283	2169.8	13.3	0.0175	259.6 ± 0.1
RHF	cc-pVDZ	− 112.750151	1.1101	2431.6	10.9	0.0147	176.42
	cc-pVTZ	− 112.781813	1.1045	2425.0	11.1	0.0149	182.92
	cc-pVQZ	− 112.790626	1.1020	2427.3	11.2	0.0151	184.36
	cc-pV5Z	− 112.792412	1.1018	2426.9	11.3	0.0151	184.45
	cc-pV6Z	− 112.792649	1.1018	2426.8	11.3	0.0151	184.50
	aug-cc-pVDZ	− 112.755481	1.1108	2402.6	11.1	0.0150	177.44
	aug-cc-pVTZ	− 112.782944	1.1041	2420.7	11.1	0.0150	183.19
	aug-cc-pVQZ	− 112.790812	1.1020	2425.9	11.2	0.0151	184.39
	aug-cc-pV5Z	− 112.792463	1.1018	2426.7	11.3	0.0151	184.48
MP2	cc-pVDZ	− 113.036807	1.1472	2114.0	12.9	0.0172	253.99
	cc-pVTZ	− 113.135652	1.1385	2121.4	13.0	0.0174	264.93
	cc-pVQZ	− 113.169899	1.1346	2128.4	13.3	0.0177	269.42
	cc-pV5Z	− 113.182352	1.1341	2127.8	13.3	0.0178	270.88
	cc-pV6Z	− 113.187424	1.1339	2127.9	13.4	0.0178	271.61
	aug-cc-pVDZ	− 113.054970	1.1502	2072.3	13.1	0.0175	255.58
	aug-cc-pVTZ	− 113.142411	1.1390	2109.8	13.1	0.0176	265.83
	aug-cc-pVQZ	− 113.172923	1.1352	2123.0	13.2	0.0178	269.89
	aug-cc-pV5Z	− 113.183953	1.1343	2125.6	13.4	0.0178	271.18
MP3	cc-pVDZ	− 113.035146	1.1307	2299.7	9.8	0.0143	234.76
	cc-pVTZ	− 113.131861	1.1218	2305.9	10.2	0.0146	243.69
	cc-pVQZ	− 113.163926	1.1178	2314.5	10.4	0.0149	248.14
	cc-pV5Z	− 113.173946	1.1171	2315.2	10.5	0.0149	249.40
	cc-pV6Z	− 113.177434	1.1169	2315.8	10.5	0.0149	249.98
	aug-cc-pVDZ	− 113.052995	1.1331	2258.5	10.1	0.0146	234.91
	aug-cc-pVTZ	− 113.138231	1.1220	2296.4	10.2	0.0147	244.40
	aug-cc-pVQZ	− 113.166328	1.1182	2310.3	10.3	0.0149	248.53
	aug-cc-pV5Z	− 113.174992	1.1173	2313.9	10.5	0.0149	249.63
MP4	cc-pVDZ	− 113.059596	1.1550	1991.7	20.2	0.0217	245.98
	cc-pVTZ	− 113.161548	1.1461	2009.0	19.1	0.0215	257.27
	cc-pVQZ	− 113.194139	1.1417	2021.8	19.1	0.0216	261.88
	cc-pV5Z	− 113.204541	1.1410	2022.3	19.1	0.0216	263.29
	cc-pV6Z	− 113.208200	1.1408	2023.0	19.1	0.0216	263.92
	aug-cc-pVDZ	− 113.079063	1.1582	1953.2	19.8	0.0219	245.99
	aug-cc-pVTZ	− 113.168312	1.1466	1997.9	19.2	0.0216	257.87
	aug-cc-pVQZ	− 113.196649	1.1422	2016.5	19.1	0.0216	262.23
	aug-cc-pV5Z	− 113.205621	1.1412	2020.6	19.2	0.0217	263.50
CCSD	cc-pVDZ	− 113.043970	1.1384	2209.2	11.6	0.0157	235.73
	cc-pVTZ	− 113.138549	1.1288	2222.8	11.7	0.0160	244.46
	cc-pVQZ	− 113.169410	1.1243	2234.7	11.9	0.0163	248.67
	cc-pV5Z	− 113.179113	1.1236	2236.1	12.0	0.0163	249.87
	cc-pV6Z	− 113.182552	1.1233	2237.1	12.1	0.0163	250.43
	aug-cc-pVDZ	− 113.061313	1.1405	2171.8	11.9	0.0161	234.96
	aug-cc-pVTZ	− 113.144520	1.1288	2215.1	11.9	0.0162	244.89
	aug-cc-pVQZ	− 113.171641	1.1246	2231.2	12.0	0.0163	248.95
	aug-cc-pV5Z	− 113.180109	1.1237	2235.2	12.1	0.0163	250.06

Table 1 Continued

Method	Basis set	E_e (a.u.)	r_e (Å)	ω_e (cm^{-1})	$\omega_e x_e$ (cm^{-1})	α_e (cm^{-1})	D_e (kcal mol^{-1})
CCSD(T)	cc-pVDZ	− 113.054976	1.1446	2144.1	12.7	0.0167	241.52
	cc-pVTZ	− 113.155579	1.1357	2153.8	12.8	0.0170	251.91
	cc-pVQZ	− 113.187906	1.1314	2164.4	13.0	0.0172	256.32
	cc-pV5Z	− 113.198188	1.1307	2165.0	13.0	0.0173	257.62
	cc-pV6Z	− 113.201832	1.1305	2165.8	13.1	0.0173	258.23
	aug-cc-pVDZ	− 113.074053	1.1473	2104.7	13.0	0.0171	240.92
	aug-cc-pVTZ	− 113.162194	1.1360	2144.5	12.9	0.0172	252.31
	aug-cc-pVQZ	− 113.190371	1.1318	2160.1	13.0	0.0173	256.60
	aug-cc-pV5Z	− 113.199276	1.1309	2163.8	13.1	0.0173	257.82

[a] Ref. [42]. The experimental D_e has been adjusted for spin–orbit effects. See the text.

isoelectronic N_2 molecule [15]. For example, D_e of CO converges smoothly from below for the icCAS + 1 + 2 and CCSD(T) methods with the resulting CBS limits agreeing to within 1 kcal mol^{-1} of experiment. The Møller–Plesset series, on the other hand, displays even larger errors than were observed previously for N_2 but with the same pattern, i.e., D_e(MP2) converges to a value that is much too large (+ 12.4 kcal mol^{-1}), D_e(MP3) is too small (−8.7 kcal mol^{-1}), and D_e(MP4) is too large but with less than half the error as the MP2 result (+4.8 kcal mol^{-1}). The CCSD method predicts a D_e essentially identical to that obtained with the MP3 method.

As can be seen, D_e(MP2) with the cc-pVDZ/cc-pVTZ sets and D_e(MP4) with the cc-pVTZ/cc-pVQZ sets are in fortuitously good agreement with the experimental value (such points were also observed in the calculations on N_2). In the absence of a knowledge of the dependence of the calculated D_e values on the basis set, this agreement could be construed to imply that these methods are far more

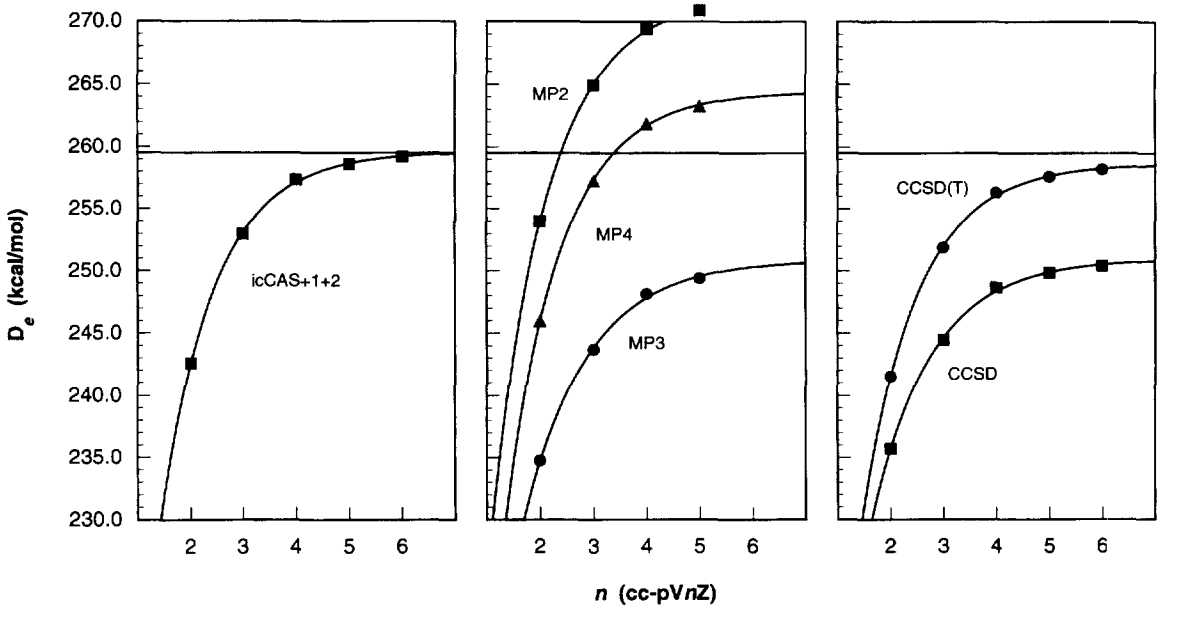

Fig. 1. Calculated equilibrium dissociation energies for CO as a function of correlation consistent basis set, cc-pVDZ–cc-pV6Z. The horizontal solid line is the experimental value of 259.6 kcal mol^{-1}. The lines connecting the points are exponential fits to the data.

Table 2
Calculated spectroscopic constants of CO compared with experiment. Methods based on multiconfigurational wave functions

Method	Basis set	E_e (a.u.)	r_e (Å)	ω_e (cm^{-1})	$\omega_e x_e$ (cm^{-1})	α_e (cm^{-1})	D_e (kcal mol^{-1})
Experimental			1.1283	2169.8	13.3	0.0175	259.6 ± 0.1
CASSCF	cc-pVDZ	− 112.880710	1.1419	2165.0	12.5	0.0165	246.13
	cc-pVTZ	− 112.911583	1.1355	2165.7	12.5	0.0167	251.13
	cc-pVQZ	− 112.920363	1.1328	2169.4	12.7	0.0169	252.29
	cc-pV5Z	− 112.922181	1.1326	2169.2	12.7	0.0169	252.35
	cc-pV6Z	− 112.922419	1.1326	2169.1	12.7	0.0169	252.38
	aug-cc-pVDZ	− 112.886181	1.1426	2141.9	12.7	0.0168	246.94
	aug-cc-pVTZ	− 112.912691	1.1351	2162.5	12.7	0.0168	251.21
	aug-cc-pVQZ	− 112.920567	1.1329	2168.4	12.7	0.0169	252.27
	aug-cc-pV5Z	− 112.922237	1.1326	2169.1	12.8	0.0169	252.36
CAS + 1 + 2	cc-pVDZ	− 113.048820	1.1448	2140.9	12.9	0.0169	242.57
	cc-pVTZ	− 113.142689	1.1354	2155.5	13.0	0.0171	252.99
	cc-pVQZ	− 113.172875	1.1309	2167.6	13.1	0.0173	257.35
	cc-pV5Z	− 113.182400	1.1302	2169.1	13.2	0.0173	258.61
	cc-pV6Z	− 113.185768	1.1300	2170.0	13.2	0.0173	259.19
	aug-cc-pVDZ	− 113.065796	1.1469	2105.7	13.2	0.0172	242.74
	aug-cc-pVTZ	− 113.148430	1.1354	2148.2	13.1	0.0172	253.62
	aug-cc-pVQZ	− 113.175029	1.1312	2164.3	13.2	0.0173	257.69
	aug-cc-pV5Z	− 113.183369	1.1303	2168.1	13.2	0.0173	258.82
CAS + 1 + 2 + Q	cc-pVDZ	− 113.057014	1.1455	2136.1	12.9	0.0169	241.63
	cc-pVTZ	− 113.155799	1.1363	2148.4	13.0	0.0171	251.81
	cc-pVQZ	− 113.187472	1.1319	2159.8	13.2	0.0173	256.22
	cc-pV5Z	− 113.197431	1.1312	2161.0	13.2	0.0174	257.52
	cc-pV6Z	− 113.200942	1.1310	2161.8	13.2	0.0174	258.11
	aug-cc-pVDZ	− 113.075758	1.1481	2096.8	13.2	0.0173	241.05
	aug-cc-pVTZ	− 113.162156	1.1365	2139.6	13.1	0.0173	252.26
	aug-cc-pVQZ	− 113.189816	1.1323	2155.7	13.2	0.0174	256.52
	aug-cc-pV5Z	− 113.198459	1.1314	2159.6	13.2	0.0174	257.71

accurate than the converged results indicate. Clearly, the use of systematically convergent basis sets such as the cc-pV*n*Z family is critical to an unambiguous determination of the inherent accuracies of different correlation methods.

Similar basis set convergence patterns are observed in Tables 1 and 2 and Fig. 2 for the equilibrium separation. The icCAS + 1 + 2 and CCSD(T) methods converge smoothly from above to values slightly longer (0.002 Å) than the experimental value. The effect of approximately adding triple excitations to the CCSD method increases r_e by 0.007 Å. With the cc-pV6Z basis set, which is expected to yield r_e values very close to the basis set limit, the remaining or intrinsic errors in these methods are just + 0.0017 Å, + 0.0027 Å, and + 0.0022 Å for icCAS + 1 + 2, icCAS + 1 + 2 + Q, and CCSD(T) respectively. The results for the MP*n* series are much less satisfactory. Specifically, with the cc-pV6Z basis set, the MP2 r_e is longer than experiment by 0.0056 Å, MP3 is too short by 0.0114 Å, and MP4 is too long by 0.0125 Å. Hence, the same oscillatory behavior as discussed previously for D_e is also present for r_e, but in this case the MP*n* expansion does not appear to be converging, i.e., the error at the MP4 level is much larger than that at the MP2 level! This statement is true even when the core electrons are included in the calculations; see below. Analogous behavior has been previously observed for both N_2 and HF [6,13,15].

The harmonic vibrational frequencies ω_e depicted in Fig. 3 closely parallel the results for r_e. Again the

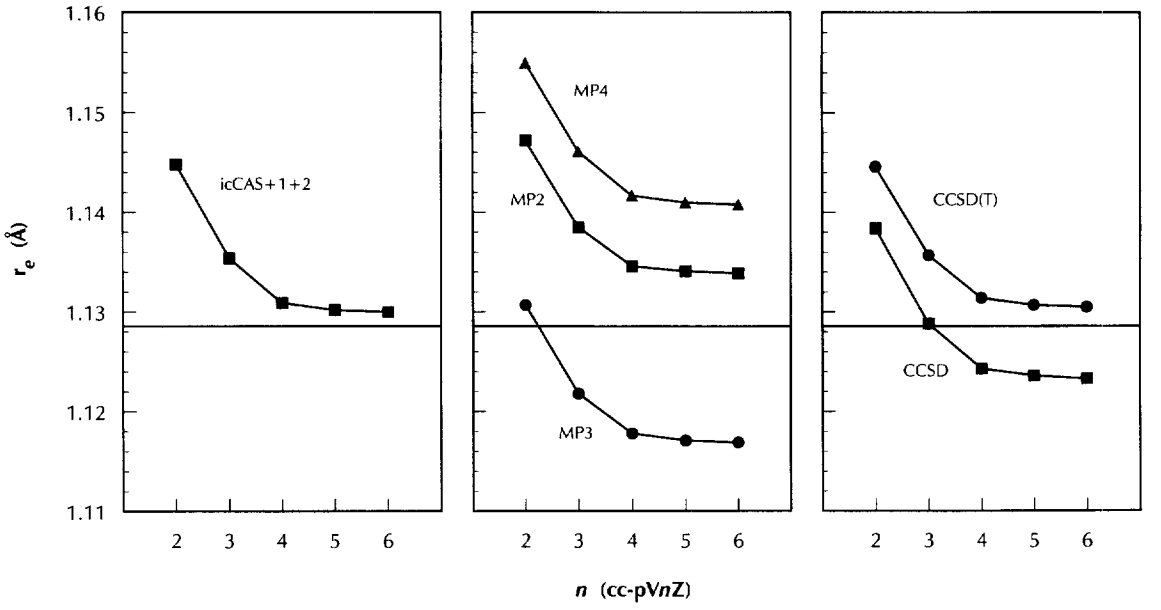

Fig. 2. Calculated equilibrium bond distances for CO as a function of correlation consistent basis set. The horizontal solid line is the experimental value of 1.1283 Å.

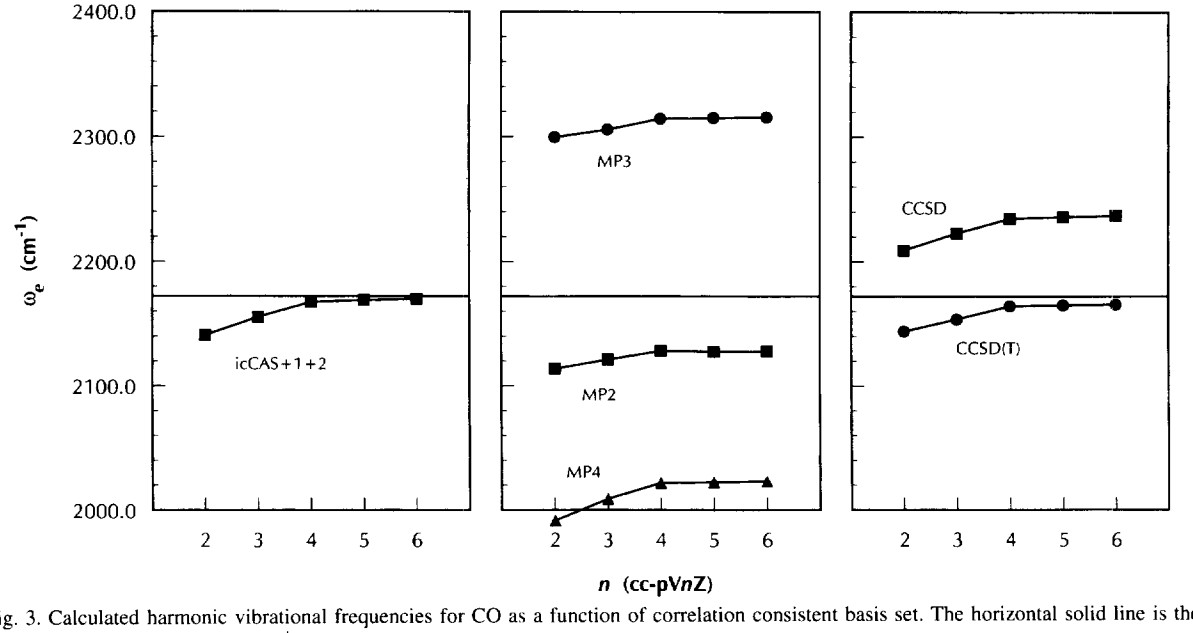

Fig. 3. Calculated harmonic vibrational frequencies for CO as a function of correlation consistent basis set. The horizontal solid line is the experimental value of 2169.8 cm^{-1}.

icCAS + 1 + 2 and CCSD(T) methods yield similarly accurate results and in this case smoothly converge with basis set from below. Near the basis set limit with the cc-pV6Z basis set, the remaining errors in ω_e are just + 0.2, − 8.0, and − 4.0 cm^{-1} for icCAS + 1 + 2, icCAS + 1 + 2 + Q, and CCSD(T) respectively. For the perturbation theory methods, both MP2 and MP4 yield values for ω_e that are much smaller than experiment (− 41.9 and − 146.8 cm^{-1}, respectively), which correlates with the overestimation of r_e by both. Again, the Møller–Plesset perturbation expansion does not appear to be converging.

Also shown in Tables 1 and 2 are the computed values for the vibrational anharmonicity, $\omega_e x_e$. As might be expected from the previous results, the CASSCF method provides a substantial improvement over the HF method. In the correlated calculations, see Fig. 4, the CCSD(T) method yields results for $\omega_e x_e$ very similar to that of the multireference CI method, which in turn is very close to the experimental value. In contrast to the other spectroscopic constants, the basis set dependence of this quantity is not large and it is essentially converged at the cc-pVQZ level. Since the anharmonicity is determined principally by the higher derivatives of the potential energy function, inadequacies in the correlation method can be accentuated. This is certainly the case with CO, where the MP4 value for $\omega_e x_e$ is nearly 50% larger than experiment, 19.1 versus 13.3 cm^{-1} with the cc-pV6Z basis set. Casting further doubt on the convergence of the MP*n* series for this species, the errors in both $\omega_e x_e$ (MP2) and $\omega_e x_e$ (MP3) are much smaller than in $\omega_e x_e$ (MP4).

3.1.2. Augmented sets

While the extra diffuse functions included in the aug-cc-pV*n*Z sets are not expected to have a large effect on the spectroscopic constants of a neutral molecule like CO, the role of these functions has also been investigated. The calculated spectroscopic constants obtained with these sets are summarized in Tables 1 and 2 and the results for D_e, r_e, and ω_e are compared with the cc-pV*n*Z values in Fig. 5 for the CCSD(T) method. In general, the changes due to the additional diffuse functions are very small and decrease dramatically with basis set size. At the V5Z level, the effects due to diffuse functions are just + 0.2 kcal mol^{-1}, + 0.0002 Å, and − 1.2 cm^{-1} for D_e, r_e, and ω_e, respectively. As seen in Fig. 5, the

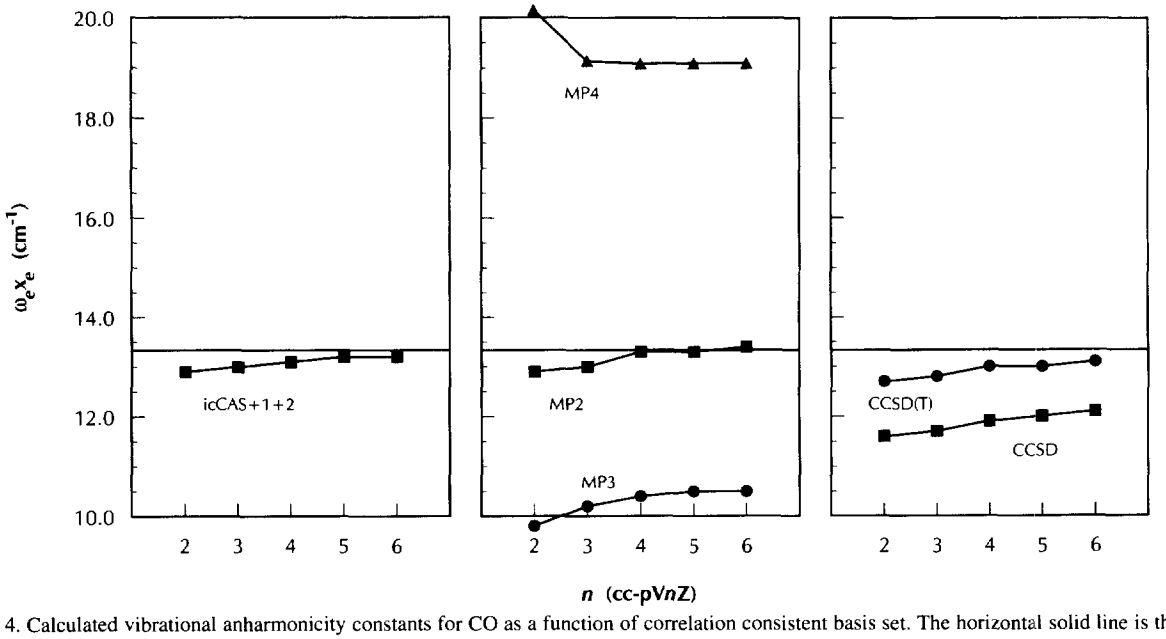

Fig. 4. Calculated vibrational anharmonicity constants for CO as a function of correlation consistent basis set. The horizontal solid line is the experimental value of 13.3 cm^{-1}.

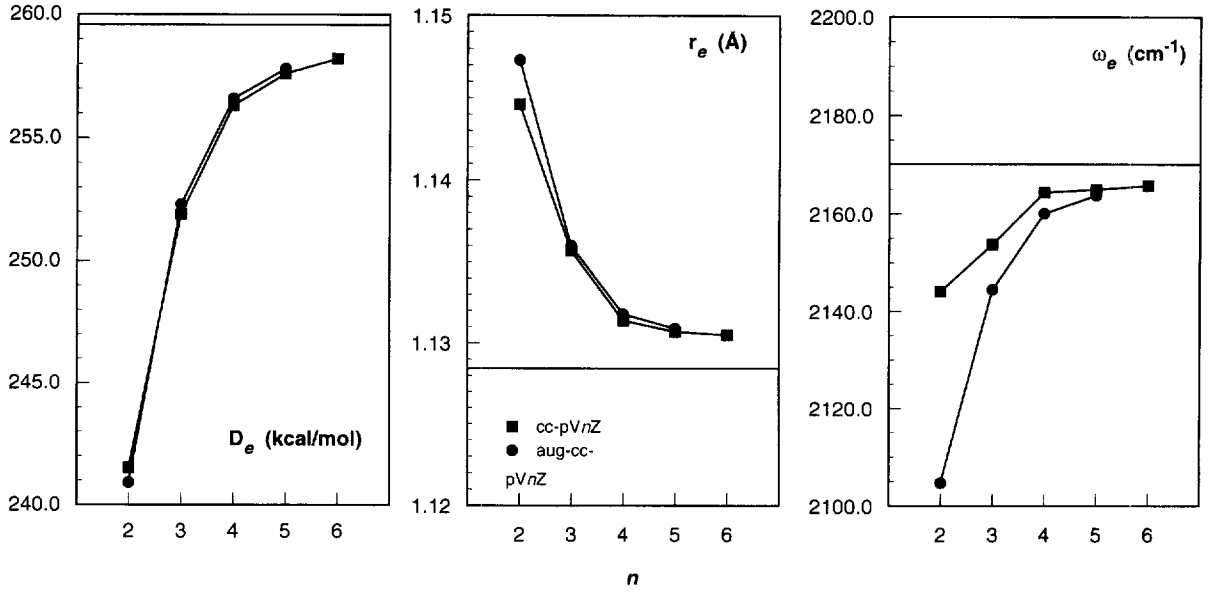

Fig. 5. CCSD(T) values of D_e, r_e, and ω_e as a function of both the cc-pVnZ and aug-cc-pVnZ basis sets. The horizontal solid lines are the experimental values.

largest differences are at the VDZ level for ω_e where the aug-cc-pVDZ result is nearly 40 cm^{-1} smaller than the cc-pVDZ value. However, while the value of ω_e calculated with the aug-cc-pVDZ set is much further from experiment, it yields a smoother overall convergence pattern when viewed in the context of the results for $n > 2$.

3.1.3. Complete basis set limits

As noted in previous benchmarking studies, the systematic convergence behavior of the correlation consistent basis sets can be exploited to yield estimates of the complete basis set (CBS) limit for a given property. Table 3 shows the CBS limits estimated for E_e, D_e, r_e, and ω_e. Those for the minimum

Table 3
Estimated complete basis set (CBS) limits from valence-only calculations compared with experiment

Method	E_e [a] (a.u.)	D_e [a] (kcal mol^{-1})	r_e [b] (Å)	ω_e [b] (cm^{-1})
Experimental [c]		259.6 ± 0.1	1.1283	2169.8
SCF	− 112.7931	184.5	1.1018	2427
CASSCF	− 112.9229	252.4	1.1326	2169
MP2	− 113.1894	272.0	1.1339	2128
MP3	− 113.1791	250.5	1.1169	2316
MP4	− 113.2097	264.3	1.1408	2023
CCSD	− 113.1840	250.9	1.1233	2237
CCSD(T)	− 113.2033	258.6	1.1305	2166
icCAS + 1 + 2	− 113.1871	259.5	1.1300	2170
icCAS + 1 + 2 + Q	− 113.2024	258.5	1.1310	2162

[a] CBS limits obtained by exponential extrapolation of the cc-pVDZ through cc-pV6Z results. See the text.
[b] These estimated CBS limits correspond to the cc-pV6Z results.
[c] Ref. [42].

total energy E_e and the dissociation energy D_e were obtained by the exponential extrapolation procedure described above (cc-pVDZ-cc-pV6Z results), while those for the equilibrium separation r_e and the harmonic frequency ω_e correspond to the cc-pV6Z values given in Tables 1 and 2. Our estimated uncertainties based on the quality of the fits are $\pm$ 0.0004 a.u. for E_e and $\pm$ 0.2 kcal mol^{-1} for D_e. In general, the effects of the extrapolation are minor, e.g., at the CCSD(T) level of theory D_e is estimated to increase by less than 0.4 kcal mol^{-1} over the cc-pV6Z result. This is somewhat less than what was found for N_2, where the difference between the CCSD(T) D_e with the cc-pV6Z basis set and at the CBS limit was 0.6 kcal mol^{-1}.

As discussed above, once the CBS limits have been estimated, the intrinsic error or inherent accuracy of each correlation method can be unambiguously compared, since the coupling between the n-particle and one-particle basis set is removed. Based on the above discussion and the values shown in Table 3, the MPn methods are seen to suffer from very large intrinsic errors for CO. In addition, for the three levels of perturbation theory, the lowest order theory (MP2) has the smallest intrinsic errors! This casts considerable doubt on the efficacy of the Møller–Plesset perturbation expansion for treating electron correlation effects, at least in CO. Both CCSD(T) and icCAS + 1 + 2 (including + Q) result in very small intrinsic errors, or in other words have high inherent accuracy. For example, the CCSD(T) intrinsic errors amount to just -1.0 kcal mol^{-1} in D_e, + 0.0022 Å in r_e, and -4 cm^{-1} in ω_e. The CCSD(T) intrinsic error for D_e can be compared with the value estimated previously [6] for isoelectronic N_2 at the same level of theory, -1.6 kcal mol^{-1}.

The difference between D_e at the CBS limit and that computed with the cc-pVDZ set, ΔD_e, is an overall measure of the effect of basis set on the correlation method. For CO, the MP4 and MP2 methods have the largest basis set effects, with ΔD_e values of 18.4 and 18.0 kcal mol^{-1}, respectively. The smallest effects are for the CCSD (15.3 kcal mol^{-1}) and MP3 (16.1 kcal mol^{-1}) methods, with the icCAS + 1 + 2 (17.0 kcal mol^{-1}) and CCSD(T) (17.1 kcal mol^{-1}) methods lying in between. Although the trends are the same as in N_2, the magnitude of ΔD_e for CO is smaller by 8.4 to 9.8 kcal mol^{-1}.

3.1.4. Core/core–valence correlation effects

Of the deficiencies remaining in the theoretical treatment after extrapolating to the CBS limit, e.g., relativistic effects, core/core–valence correlation, and a more accurate treatment of the electron correlation problem (larger multireference functions, CCSDT, etc.), the largest error is expected to arise from neglect of core/core–valence correlation effects. To quantify this effect, potential energy functions from both valence-only and all-electron calculations have been determined with a series of basis sets designed specifically for describing core and core–valence correlation effects, the cc-pCVnZ sets. Both the CCSD(T) and icACPF methods were used. The results of these calculations are displayed in Table 4, as well as in Fig. 6, and show excellent convergence with respect to increases in the size of the basis set. In particular, the calculated core/core–valence correlation differential effects, i.e., the differences between the all-electron and valence-only results, converge in a very systematically manner, see Fig. 7. At this point it should be mentioned that a new series of correlation consistent basis sets has recently been developed [52] that recover molecular core–valence correlation effects more rapidly than the standard cc-pCVnZ sets. Details of these new sets, together with comparisons to the standard cc-pCVnZ sets, will appear elsewhere.

As shown in Table 4, both CCSD(T) and icACPF yield comparable values for this effect. Similar observations have been made previously for N_2, O_2, and F_2 [16,28]. Taking the icACPF values as the most reliable estimates, the estimated differences at the extrapolated CBS limits are: $\Delta E_e = 118mE_h$, $\Delta D_e = +0.95$ kcal mol^{-1}, $\Delta r_e = -0.0026$ Å, $\Delta\omega_e = +9.9$ cm^{-1}, and $\Delta\omega_e x_e = +0.05$ cm^{-1}. The effect on the vibration–rotation interaction constant a_e is found to be negligible (< 0.0001 cm^{-1}). The effects of core correlation on the spectroscopic constants of CO have recently been reported by Császár and Allen[30] using the CCSD(T) method. Their quoted results for ΔD_e, Δr_e, and $\Delta\omega_e$ are in very good agreement with the values obtained in the present work.

If we combine the above calculated core/core–valence correlation effects with the CBS limits in Table 3, we obtain intrinsic errors for all-electron CCSD(T) calculations of just -0.1 kcal mol^{-1} (D_e), -0.0004 Å (r_e), and +6 cm^{-1} (ω_e). Application of

Table 4
Calculated effects of correlating the 1s-core electrons using CCSD(T), ACPF, and the core–valence correlation consistent basis sets

Method	Basis set	E_e (a.u.)	r_e (Å)	ω_e (cm^{-1})	$\omega_e x_e$ (cm^{-1})	α_e (cm^{-1})	D_e (kcal mol^{-1})
CCSD(T)							
10 e-'s	cc-pCVDZ	− 113.059983	1.1435	2143.84	12.83	0.0168	242.10
	cc-pCVTZ	− 113.161153	1.1343	2155.77	12.91	0.0171	252.51
	cc-pCVQZ	− 113.190193	1.1311	2164.51	13.07	0.0173	256.45
	cc-pCV5Z	− 113.199186	1.1306	2165.30	13.11	0.0173	257.69
14 e-'s	cc-pCVDZ	− 113.134711	1.1429	2146.77	12.83	0.0168	242.55
	cc-pCVTZ	− 113.264151	1.1326	2163.12	12.95	0.0171	253.27
	cc-pCVQZ	− 113.303351	1.1289	2173.84	13.12	0.0173	257.33
	cc-pCV5Z	− 113.315390	1.1282	2175.14	13.15	0.0174	258.63
Δ	cc-pCVDZ	− 0.0747	− 0.0006	2.93	0.00		0.45
	cc-pCVTZ	− 0.1030	− 0.0017	7.35	0.04		0.76
	cc-pCVQZ	− 0.1132	− 0.0022	9.33	0.05		0.88
	cc-pCV5Z	− 0.1162	− 0.0024	9.84	0.04		0.93
	Est CBS limit	− 0.118	− 0.0026	10.4			0.96
ACPF							
10 e-'s	cc-pCVDZ	− 113.060560	1.1442	2136.97	12.96	0.0169	242.32
	cc-pCVTZ	− 113.159196	1.1347	2151.43	13.02	0.0172	252.52
	cc-pCVQZ	− 113.187486	1.1315	2160.85	13.17	0.0174	256.42
	cc-pCV5Z	− 113.196178	1.1310	2161.96	13.20	0.0174	257.62
14 e-'s	cc-pCVDZ	− 113.135204	1.1436	2139.62	12.96	0.0169	242.70
	cc-pCVTZ	− 113.262054	1.1330	2158.35	13.05	0.0172	253.22
	cc-pCVQZ	− 113.300458	1.1293	2169.67	13.22	0.0174	257.26
	cc-pCV5Z	− 113.312182	1.1286	2171.33	13.25	0.0174	258.52
Δ	cc-pCVDZ	− 0.0746	− 0.0006	2.65	0.00		0.38
	cc-pCVTZ	− 0.1029	− 0.0017	6.92	0.03		0.70
	cc-pCVQZ	− 0.1130	− 0.0022	8.82	0.05		0.84
	cc-pCV5Z	− 0.1160	− 0.0024	9.37	0.05		0.90
	Est CBS limit	− 0.118	-0.0026	9.9			0.95

the predicted 1s correlation effects to the valence-only intrinsic errors for the icCAS + 1 + 2 + Q method yields somewhat smaller all-electron intrinsic errors of –0.2 kcal mol^{-1} (D_e), +0.0001 Å (r_e), and + 2 cm^{-1} (ω_e).

Note that inclusion of core and core–valence correlation effects would not alter the conclusion drawn earlier about the convergence (or lack thereof) of the MP*n* perturbation theory expansion.

3.2. Dipole and quadrupole moments

3.2.1. Dipole moment

When discussing the early successes and failures of quantum chemistry, one of the most famous examples of the latter was the incorrect prediction of the dipole moment *polarity* of CO by the Hartree–Fock method. In 1958, Rosenblum et al. [53] carried out microwave experiments on the rotational magnetic moments of CO that indicated a polarity of C^-O^+ for the electric dipole moment. In the early 1960s, Hartree–Fock calculations, which were substantial undertakings at that time, were carried out first by Nesbet [54] and then by Huo [55] to confirm the experimental result. While the magnitude of the computed dipole moments, –0.379 D by Nesbet and –0.274 D by Huo, were consistent with the experimental value of that time, 0.112 D by Burrus [56], the calculated polarities were opposite to that of Rosenblum et al. [53] To address questions raised concerning the interpretation

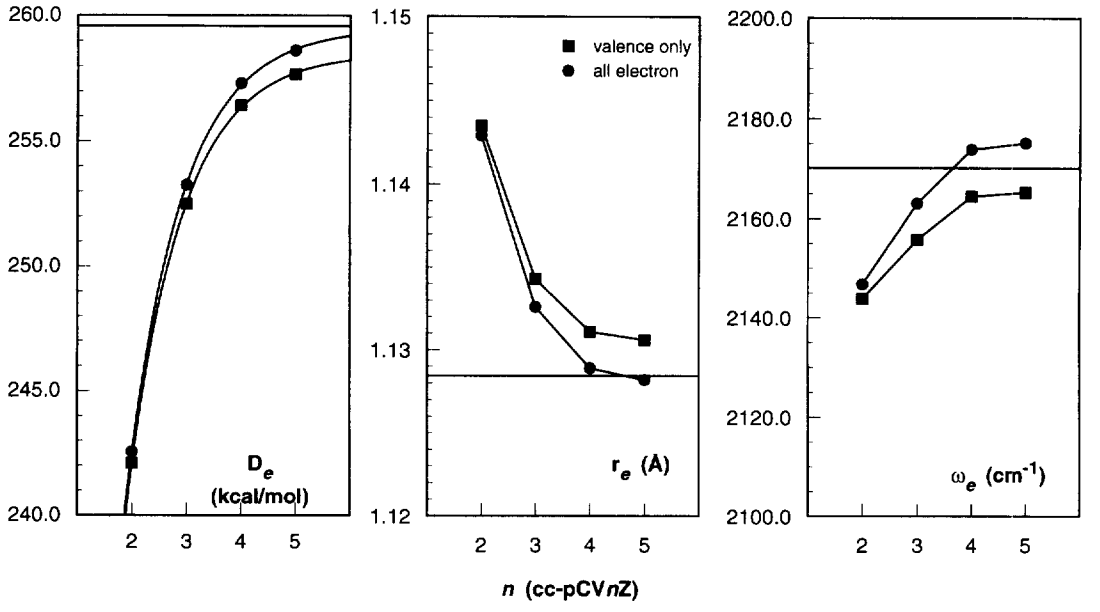

Fig. 6. Convergence of D_e, r_e, and ω_e for both valence-only and all-electron correlation at the CCSD(T) level of the theory for the core–valence cc-pCVnZ basis sets. The horizontal solid lines are the experimental values.

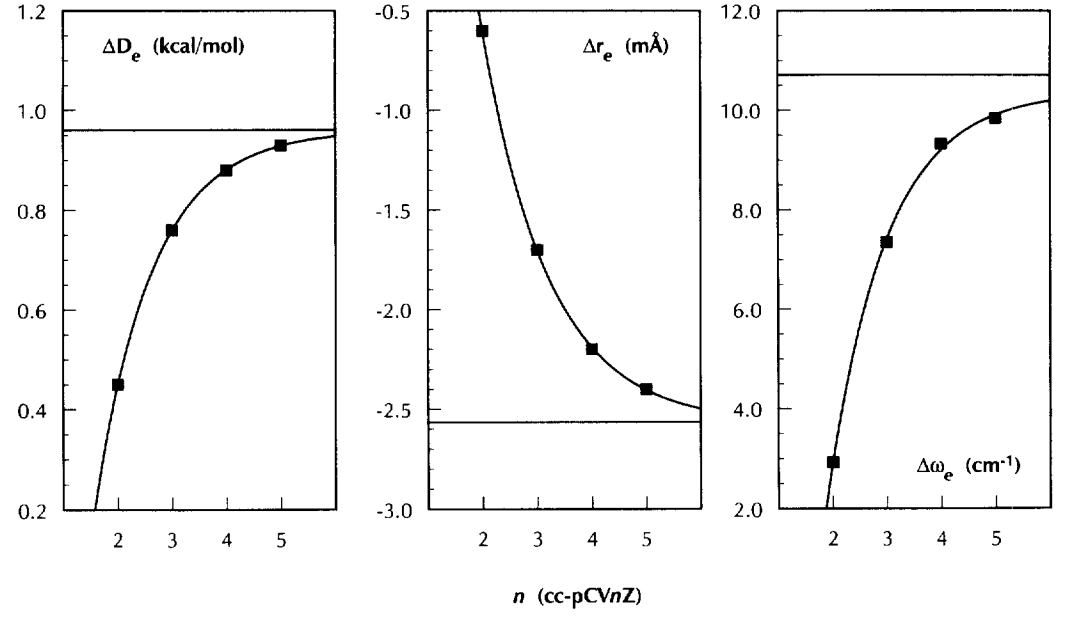

Fig. 7. Contributions to D_e, r_e, and ω_e of correlating the 1s-like electrons as a function of the cc-pCVnZ basis sets. The lines connecting the points are exponential fits to the data, and the horizontal lines are the extrapolated values for $n \rightarrow \infty$.

of the experimental data, more accurate experiments were carried out by Ozier et al. [57,58] a few years later, but an unambiguous determination of the dipole moment sign was not obtained.

The controversy persisted until 1974 when Billingsley and Krauss [59] carried out correlated calculations at the configuration interaction level of theory that yielded a dipole moment of + 0.151 D, reproducing the experimental polarity indicated by the earlier work, and vindicating modern quantum chemistry. This theoretical result was followed a few years later by the molecular beam electric resonance experiments of Meerts et al. [50], where the polarity of CO was unambiguously determined to be C^-O^+. It is now known, of course, that the difficulty in accurately computing the dipole moment of CO is mainly due to two factors: (i) substantial sensitivity of the computed dipole moment to the degree of electron correlation included in the calculations and (ii) the strong variation of the dipole moment with the internuclear distance ($d\mu/dr = -3.218$ D Å^{-1}) with μ changing sign near the equilibrium separation.

Of the numerous calculations of the equilibrium dipole moment of CO, the most accurate values include those from the MRCI calculations of Feller et al. (0.102 D) [60], the CCSD(T) results of Scuseria et al. (0.122 D) and Botschwina et al. (0.125 D) [62], the ACPF results of Ernzerhof et al. (0.113 D) [45], and the more recent QCISD(T) and CCSD(T) values of Luis et al. (0.126 D) [63] and Maroulis (0.131 D) [64], respectively. These can be compared with the experimental equilibrium values (μ_e) of 0.1222 D by Muenter [49] and 0.123(2) D determined by Meerts et al. [50]. The rotationless value in $v=0$, 0.10980(3) D, has been accurately determined from the molecular beam experiments of Muenter [49]. Theoretical dipole moment functions (DMFs) have also been determined by Werner [65], Cooper and Kirby [66], and most recently by Langhoff and Bauschlicher [44]. The latter work used large ACPF wave functions in conjunction with an aug-cc-pVQZ basis set to determine a global DMF that accurately reproduced experiment for both the low-lying permanent dipole moments and rotationless dipole moment matrix elements for transitions from $v=0$.

In the present work, dipole moments have been calculated with each correlation method and basis set, including doubly augmented sets, at the experimental equilibrium separation of $2.1322a_0$ [42]. These results are shown in Tables 5and 6. Each theoretical

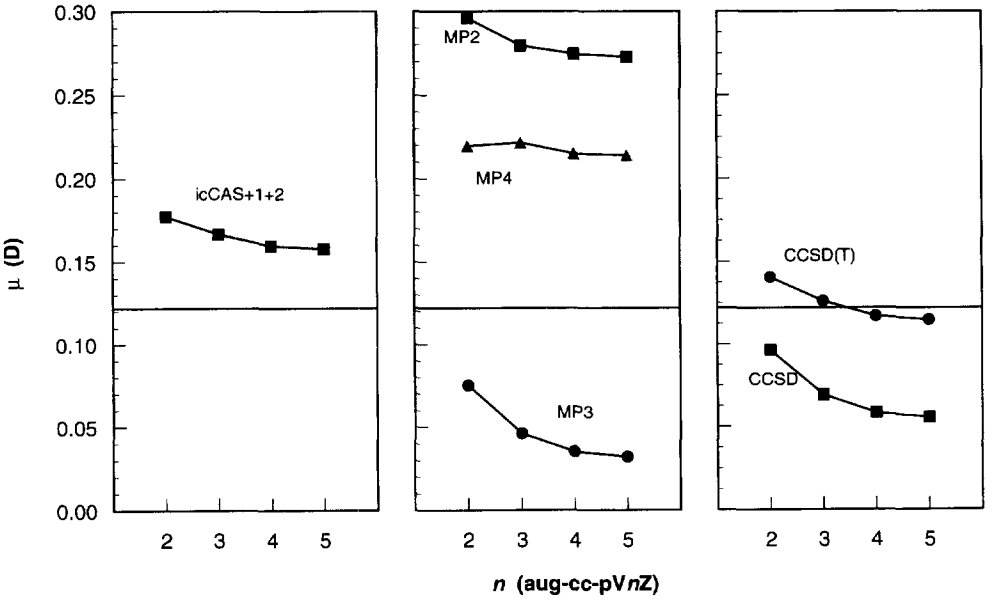

Fig. 8. Calculated values of the equilibrium dipole moment as a function of the aug-cc-pV*n*Z basis sets. The horizontal solid line is the experimental value.

Table 5
Calculated dipole moments, quadrupole moments, and dipole polarizabilities (in a.u.) of CO compared to experiment (at $r = 2.1322a_0$). Methods based on a single configuration wave function

Method	Basis set	μ_e	Θ_e	$(\alpha_{zz})_e$	$(\alpha_{xx})_e$	$\bar{\alpha}$	$\Delta\alpha$
Experimental		0.0481 [a]	− 1.45 ± 0.03 [b]			13.04 [c]	3.54 [d]
SCF	aug-cc-pVDZ	− 0.1022	− 1.582	14.423	10.955	12.111	3.468
	aug-cc-pVTZ	− 0.1052	− 1.546	14.492	11.225	12.314	3.266
	aug-cc-pVQZ	− 0.1045	− 1.530	14.481	11.270	12.340	3.211
	aug-cc-pV5Z	− 0.1044	− 1.530	14.470	11.271	12.337	3.200
	d-aug-cc-pVDZ	− 0.0987	− 1.543	14.479	11.247	12.324	3.233
	d-aug-cc-pVTZ	− 0.1043	− 1.534	14.490	11.273	12.346	3.217
	d-aug-cc-pVQZ	− 0.1043	− 1.530	14.471	11.274	12.339	3.198
MP2	aug-cc-pVDZ	0.1165	− 1.571	15.632	11.676	12.995	3.956
	aug-cc-pVTZ	0.1100	− 1.509	15.635	11.930	13.165	3.704
	aug-cc-pVQZ	0.1081	− 1.492	15.596	11.956	13.169	3.640
	aug-cc-pV5Z	0.1074	− 1.490	15.569	11.949	13.156	3.621
	d-aug-cc-pVDZ	0.1192	− 1.541	15.726	11.983	13.230	3.743
	d-aug-cc-pVTZ	0.1108	− 1.499	15.650	11.990	13.210	3.660
	d-aug-cc-pVQZ	0.1082	− 1.491	15.594	11.967	13.176	3.626
MP3	aug-cc-pVDZ	0.0296	− 1.526	15.281	11.394	12.690	3.886
	aug-cc-pVTZ	0.0181	− 1.462	15.223	11.622	12.822	3.602
	aug-cc-pVQZ	0.0139	− 1.444	15.164	11.637	12.813	3.527
	aug-cc-pV5Z	0.0126	− 1.443	15.133	11.625	12.794	3.508
	d-aug-cc-pVDZ	0.0323	− 1.491	15.365	11.694	12.918	3.672
	d-aug-cc-pVTZ	0.0190	− 1.452	15.230	11.674	12.859	3.556
	d-aug-cc-pVQZ	0.0141	− 1.444	15.157	11.642	12.814	3.516
MP4	aug-cc-pVDZ	0.0864	− 1.583	15.502	11.668	12.946	3.834
	aug-cc-pVTZ	0.0872	− 1.524	15.496	11.908	13.104	3.587
	aug-cc-pVQZ	0.0846	− 1.507	15.446	11.926	13.099	3.520
	aug-cc-pV5Z	0.0842	− 1.505	15.418	11.916	13.084	3.502
	d-aug-cc-pVDZ	0.0895	− 1.553	15.596	11.962	13.173	3.634
	d-aug-cc-pVTZ	0.0880	− 1.515	15.506	11.963	13.144	3.543
	d-aug-cc-pVQZ	0.0847	− 1.506	15.441	11.934	13.103	3.508
CCSD	aug-cc-pVDZ	0.0379	− 1.534	15.528	11.514	12.852	4.014
	aug-cc-pVTZ	0.0272	− 1.476	15.433	11.712	12.952	3.722
	aug-cc-pVQZ	0.0229	− 1.459	15.370	11.721	12.938	3.649
	aug-cc-pV5Z	0.0218	− 1.457	15.338	11.708	12.918	3.630
	d-aug-cc-pVDZ	0.0406	− 1.501	15.613	11.808	13.076	3.805
	d-aug-cc-pVTZ	0.0280	− 1.466	15.440	11.763	12.989	3.677
	d-aug-cc-pVQZ	0.0231	− 1.459	15.365	11.727	12.940	3.638
CCSD(T)	aug-cc-pVDZ	0.0553	− 1.540	15.607	11.649	12.968	3.958
	aug-cc-pVTZ	0.0496	− 1.481	15.538	11.860	13.086	3.679
	aug-cc-pVQZ	0.0460	− 1.462	15.480	11.873	13.076	3.606
	aug-cc-pV5Z	0.0451	− 1.461	15.449	11.862	13.057	3.587

Table 5 Continued

Method	Basis set	μ_e	Θ_e	$(\alpha_{zz})_e$	$(\alpha_{xx})_e$	$\bar{\alpha}$	$\Delta\alpha$
	d-aug-cc-pVDZ	0.0581	− 1.509	15.700	11.946	13.197	3.754
	d-aug-cc-pVTZ	0.0505	− 1.471	15.548	11.915	13.126	3.633
	d-aug-cc-pVQZ	0.0461	− 1.462	15.475	11.881	13.079	3.595

[a] Ref. [49]. Also, $\mu_e = 0.0484 \pm 0.0008$ a.u. [50].
[b] Based on the $v = 0$ value (−1.44 ± 0.03 a.u.) of Meerts et al. [50].
[c] Based on the $v = 0$ value (13.0891 a.u.) of Parker and Pack [69].
[d] Equilibrium value at 488 nm from Asawaroengchai and Rosenblatt [72]. Other values in $v = 0$ at 632.8 nm include 3.59 ± 0.07 [70], 3.58 ± 0.13 [71] and 3.66 ± 0.13 [73].

method, except MP4 (!), exhibits well-behaved convergence toward the CBS limits, see Fig. 8. At the SCF level, our most accurate values (−0.1043 to −0.1044 a.u. or −0.2651 to −0.2654 D) can be compared with the numerical HF result of Sundholm et al. [51] of −0.1042 a.u. (−0.2648 D) computed at $r = 2.132a_0$. The second shell of diffuse functions is observed in Tables 5 and 6 to increase the magnitude of the dipole moment by just 0.001 a.u. (0.0025 D) at the VTZ level. This does suggest, however, that the

Table 6
Calculated dipole moments, quadrupole moments, and dipole polarizabilities (in a.u.) of CO compared with experiment (at $r = 2.1322a_0$). Methods based on a multiconfigurational wave function

Method	Basis set	μ	Θ	α_{zz}	α_{xx}	$\bar{\alpha}$	$\Delta\alpha$
Experimental [a]		0.0481	− 1.45 ± 0.03			13.04	3.54
CASSCF	aug-cc-pVDZ	0.1407	− 1.621	14.629	11.210	12.350	3.419
	aug-cc-pVTZ	0.1356	− 1.592	14.701	11.438	12.526	3.263
	aug-cc-pVQZ	0.1364	− 1.578	14.691	11.476	12.547	3.215
	aug-cc-pV5Z	0.1365	− 1.578	14.681	11.476	12.545	3.205
	d-aug-cc-pVDZ	0.1437	− 1.590	14.685	11.458	12.533	3.228
	d-aug-cc-pVTZ	0.1364	− 1.581	14.697	11.477	12.550	3.220
	d-aug-cc-pVQZ	0.1366	− 1.577	14.681	11.479	12.546	3.203
CAS-CI	aug-cc-pVDZ	0.0698	− 1.550	15.402	11.526	12.818	3.877
	aug-cc-pVTZ	0.0656	− 1.496	15.277	11.695	12.889	3.582
	aug-cc-pVQZ	0.0628	− 1.480	15.206	11.698	12.867	3.508
	aug-cc-pV5Z	0.0621	− 1.480	15.171	11.683	12.846	3.488
	d-aug-cc-pVDZ	0.0727	− 1.518	15.481	11.806	13.031	3.676
	d-aug-cc-pVTZ	0.0664	− 1.486	15.281	11.742	12.922	3.539
	d-aug-cc-pVQZ	0.0630	− 1.479	15.200	11.703	12.868	3.497
CAS-CI + Q	aug-cc-pVDZ	0.0594	− 1.536	15.634	11.644	12.974	3.990
	aug-cc-pVTZ	0.0542	− 1.478	15.521	11.832	13.062	3.690
	aug-cc-pVQZ	0.0510	− 1.461	15.453	11.839	13.043	3.614
	aug-cc-pV5Z	0.0502	− 1.461	15.418	11.825	13.023	3.593
	d-aug-cc-pVDZ	0.0622	− 1.504	15.722	11.936	13.198	3.786
	d-aug-cc-pVTZ	0.0551	− 1.468	15.529	11.884	13.099	3.645
	d-aug-cc-pVQZ	0.0512	− 1.460	15.448	11.845	13.046	3.602

[a] See the footnotes to Table 5.

change (–0.0008 a.u.) in the SCF value of μ by increasing the basis set from aug-cc-pVTZ to aug-cc-pVQZ (and further to aug-cc-pV5Z) is not due to the addition of higher angular momentum functions, but to the increasing diffuseness of the spdf functions.

As pointed out by Scuseria et al.[61], at the correlated level the higher angular momentum functions do make a nonnegligible contribution to the calculated dipole moment, e.g., the difference between d-aug-cc-pVTZ and d-aug-cc-pVQZ is 0.0044 a.u. (0.0112 D) with the CCSD(T) method. However, the second diffuse function shell has a negligible effect at the VQZ level. The effect of h-type polarization functions, as estimated by the difference between the aug-cc-pVQZ and aug-cc-pV5Z dipole moments (which also includes effects of multiple d, f, and g functions), is less than 0.001 a.u. (0.0025 D). Hence, the aug-cc-pV5Z basis set is essentially at the basis set limit for the equilibrium dipole moment of CO. The inherent accuracy (at the experimental bond distance) of the different correlation methods can now be critically evaluated by comparing the dipole moments calculated with the aug-cc-pV5Z basis set. The intrinsic error of each method (in debye) in order of decreasing magnitude (signs are relative to a positive experimental value) are (1 a.u. = 2.541748 D [67]): –0.388 (SCF), +0.225 (CASSCF), +0.151 (MP2), +0.092 (MP4), –0.090 (MP3), –0.067 (CCSD), +0.036 (icCAS + 1 + 2), –0.008 [CCSD(T)], and +0.005 (icCAS + 1 + 2 + Q).

From the CCSD(T) dipole moments obtained as a function of r, the first derivative, $(dm/dr)_e$, is calculated to be 3.245 D Å^{-1} with the aug-cc-pV5Z basis set. First derivatives of 3.208, 3.218, and 3.241 D Å^{-1} were obtained with the aug-cc-pVDZ, aug-cc-pVTZ, and aug-cc-pVQZ basis sets, respectively. Hence, the aug-cc-pV5Z value is very near the complete basis set limit for this method. This is in very good agreement with the experimental value of 3.218 D Å^{-1} and also with that obtained recently by Maroulis (3.187 D Å^{-1}). Another measure of the accuracy of our dipole moment function is the rotationless dipole moment vibrational matrix element between $v=0$ and $v=1$, which is calculated to be 0.1092 D with the aug-cc-pV5Z basis (0.1080, 0.1083, and 0.1091 D for aug-cc-pVDZ–aug-cc-pVQZ, respectively). This is also in excellent agreement with the experimental value of 0.1084 D (Ref. [68] and references therein), as well as the ACPF result of Langhoff and Bauschlicher [44], 0.1077 D. The rotationless dipole moment matrix

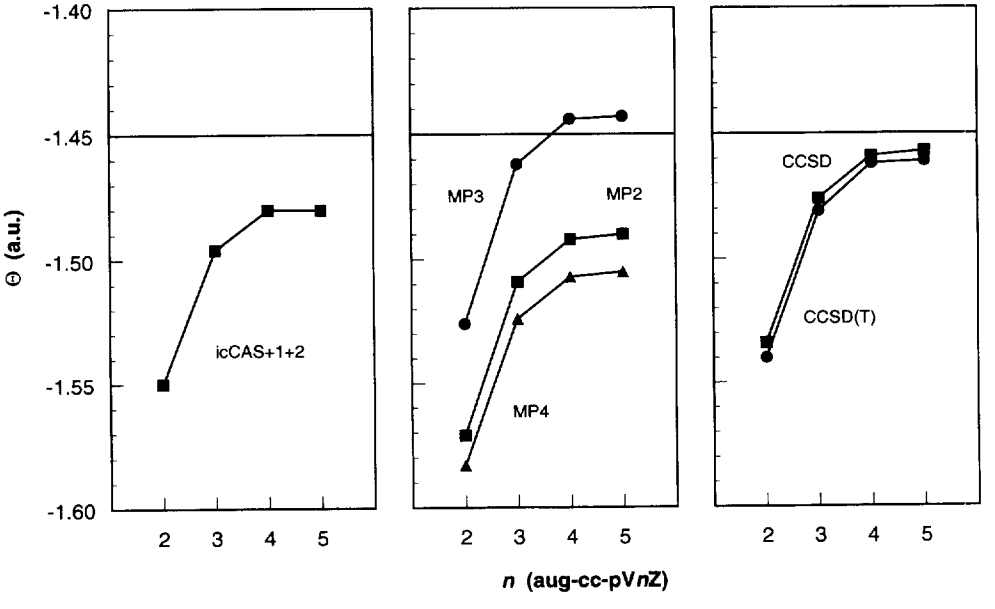

Fig. 9. Calculated values of the equilibrium molecular quadrupole moment as a function of the aug-cc-pVnZ basis sets. The horizontal solid line is the experimental value. See the text.

element can be used to derive the absolute band intensity of the 0–1 fundamental transition. The CCSD(T)/aug-cc-pV5Z value is calculated to be 413.8 km mol^{-1}, which is in excellent agreement with the experimental value of 407.8 km mol^{-1}. Lastly, the difference between our CCSD(T) μ_e and μ_0 is calculated to be -0.0132 D, which can be compared with the experimental value of -0.0125 D.

3.2.2. *Quadrupole moment*

The calculated quadrupole moments for carbon monoxide are also listed in Tables 5 and 6 and plotted in Fig. 9. In contrast to the equilibrium dipole moment, the molecular quadrupole moment is well described at the SCF level. There is, however, a somewhat stronger basis set dependence for Θ, i.e., the effect of high angular momentum functions ($l > 3$) as measured by the difference between d-aug-cc-pVTZ and d-aug-cc-pVQZ is 0.004 a.u. The extra shell of diffuse functions also has a larger effect on Θ than on μ; the difference between the d-aug-cc-pVTZ and aug-cc-pVTZ quadrupole moments is 0.022 a.u. compared with 0.001 a.u. for the dipole moment. However, at the quadruple-ζ level, these extra diffuse functions have no effect. Our calculated SCF/aug-cc-pV5Z value for Θ of -1.530 a.u. is in excellent agreement with the numerical HF value of -1.53001 au. from Sundholm et al. [51].

It is interesting to note that the CASSCF value of Θ is actually further away from the experimental value of Meerts et al. [50] than the SCF result. Inclusion of dynamic electron correlation decreases the magnitude of Θ by about 0.07 a.u. or 4.5% from the SCF value. As observed for the dipole moment, the addition of higher angular momentum polarization functions is nonnegligible at the correlated level; the quadrupole moment is lowered by 0.01 a.u. by increasing the basis set from d-aug-cc-pVTZ to d-aug-cc-pVQZ. Compared with the experimental value, the most

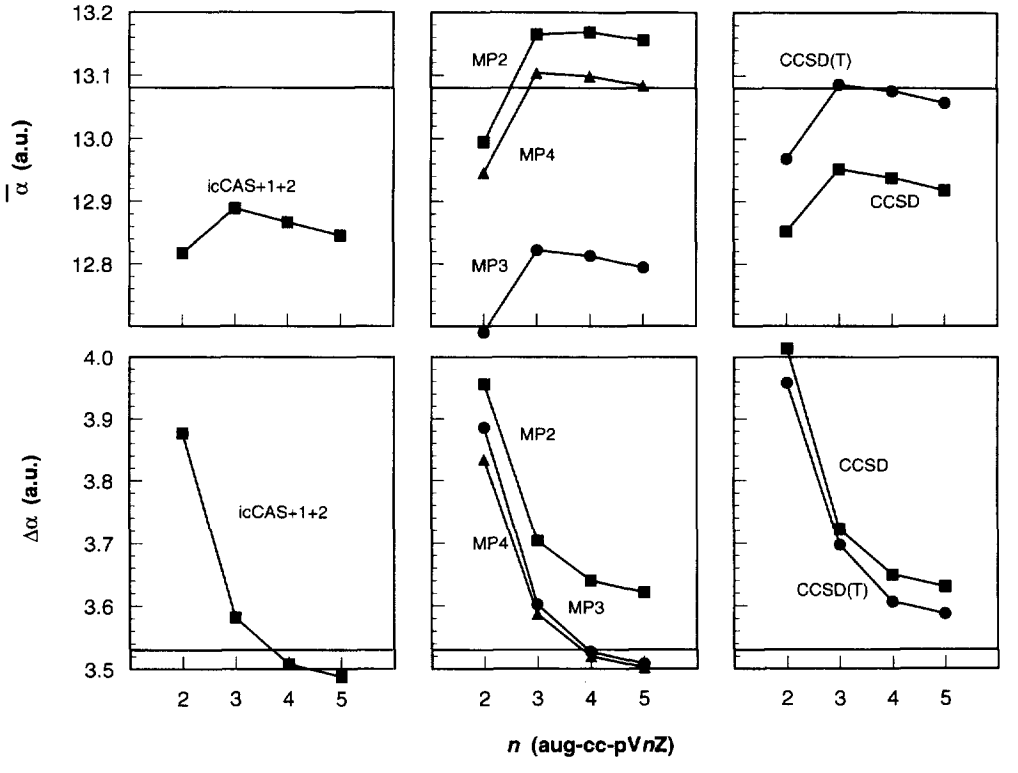

Fig. 10. Calculated values of the equilibrium isotropic ($\bar{\alpha}$) and anisotropic ($\Delta\alpha$) dipole polarizabilities for the aug-cc-pVnZ basis sets. The horizontal solid line is the experimental value. See the text.

accurate results are obtained with CCSD, CCSD(T), icCAS + 1 + 2, and icCAS + 1 + 2 + Q. The effect of triple excitations is nearly negligible for Θ (0.004 a.u.). The MP*n* series also yields good results for the quadrupole moment, but as in the case of the equilibrium bond length, the MP2 value is somewhat closer to experiment than the MP4 result.

From the CCSD(T)/aug-cc-pV5Z quadrupole moments as a function of the internuclear distance, the first derivative with respect to r (at r_e) is calculated to be 0.986 a.u. The effect of zero-point vibration on the quadrupole moment ($\Theta_{v=0} - \Theta_e$) is calculated to be 0.010 a.u., which was applied to the experimental value of Meerts et al. (-1.44 ± 0.03 a.u.) to yield the "experimental" value shown in Tables 5 and 6.

3.3. Dipole polarizabilities

The dipole polarizability components for CO, α_{zz} and α_{xx} ($\alpha_{yy} = \alpha_{xx}$), are also listed in Tables 5 and 6 for each level of theory and basis set. In addition, the average isotropic polarizability, $\bar{\alpha} = \alpha_{zz} + \alpha_{xx} + \alpha_{yy}$, and the polarizability anisotropy, $\Delta\alpha = \alpha_{zz} - \alpha_{xx}$, are included (and plotted in Fig. 10 for the aug-cc-pV*n*Z sets) and can be compared with the experimental values [69–73] for these quantities. As expected, the role of diffuse functions in the basis set is heightened for the dipole polarizability as compared with either the dipole or quadrupole moment. In general, the doubly augmented functions at the triple-ζ level have their largest effect on the perpendicular component, α_{xx}. With either the d-aug-cc-pVQZ or aug-cc-pV5Z basis set, however, the polarizabilities appear to be very close to the Hartree–Fock limit. The basis set dependence of the CASSCF polarizabilities is very similar to that of the SCF values. The CASSCF results are also not very much different from the SCF ones, hence nondynamical correlation does not play a large role in this case.

Dynamical correlation does, however, increase the dipole polarizability by about 6% as measured by the difference between the CCSD(T) and SCF values. In each case the basis set limit appears to be nearly reached with the aug-cc-pV5Z basis set, and with the doubly augmented basis sets both components converge smoothly from above (see Fig. 10). Convergence with the standard augmented sets is fairly regular for the parallel component, but less so for the perpendicular one. At the CCSD(T)/aug-cc-pV5Z level of theory, $\alpha_{zz} = 15.45$ a.u. and $\alpha_{xx} = 11.86$ a.u., which results in $\bar{\alpha} = 13.06$ a.u. and $\Delta\alpha = 3.59$ a.u. The latter quantities are in excellent agreement with experiment. In general, the MP4 method yields very similar values for the polarizability as the CCSD(T) method, although the anisotropy is somewhat lower. Our CCSD(T) results can be compared with the very recent work of Maroulis [64], who used a contracted basis set of [9s6p4d3f]. His results for the α values are nearly identical to our aug-cc-pVQZ values.

The first derivatives, $(d\alpha_{zz}/dr)_e$ and $(d\alpha_{xx}/dr)_e$, are calculated at the CCSD(T)/aug-cc-pV5Z level of theory to be 10.88 and 2.69 a.u, respectively. The analogous values for $\bar{\alpha}$ and $\Delta\alpha$ are 5.42 and 8.19 a.u., respectively. The last two values can be compared with those obtained by Maroulis [64] with CCSD(T), 5.52 and 8.28 a.u., respectively. The effects of vibrational averaging in $v = 0$ compared with equilibrium are calculated to be +0.101 a.u. (α_{zz}), +0.023 a.u. (α_{xx}), +0.049 a.u. ($\bar{\alpha}$), and +0.078 a.u. ($\Delta\alpha$) [CCSD(T)].

3.4. First and second dipole hyperpolarizabilities

The first (β) and second (γ) hyperpolarizabilities of CO are listed in Tables 7 and 8 and the results of the CCSD(T) calculations are plotted in Fig. 11 for both the aug-cc-pV*n*Z and d-aug-cc-pV*n*Z sets. In Tables 7 and 8 the static experimental values of $\bar{\beta}$ [$\bar{\beta} = 3(\beta_{zzz} + 2\beta_{zxx})/5$] and $\bar{\gamma}$ [$\bar{\gamma} = (3\gamma_{zzzz} + 8\gamma_{xxxx} + 12\gamma_{xxzz})/15$] were derived from the frequency dependent ($\lambda = 694.5$ nm) values quoted in the review of Shelton and Rice [74] by adding the SCF dispersion corrections of Sekino and Bartlett [75]. In the case of the first hyperpolarizability, the effect on the SCF values from multiple shells of diffuse functions is nonnegligible even at the quadruple-ζ level. The HF limits for β_{zzz} and β_{zxx} are estimated to be 31.4 and 4.9 a.u., respectively. The former can be compared with the limit quoted by Luis et al. [63] of 31.32 a.u. and the latter to the SCF value obtained by Maroulis [64], 4.9 a.u., with a [9s6p4d3f] basis set. Significant differences are observed for β between SCF and CASSCF. With the d-aug-cc-pVQZ basis set, the CASSCF value of $\bar{\beta}$ is nearly 1.1 a.u. larger than the SCF result. As shown in Tables 7 and 8 this is due to differences among the two components of more

Table 7
Calculated first and second hyperpolarizabilities (in a.u.) of CO compared to experiment (at $r=2.1322a_0$). Methods based on a single configuration wave function

Method	Basis set	β_{zzz}	β_{xxz}	$\bar{\beta}$	γ_{zzzz}	γ_{xxxx}	γ_{xxzz}	$\bar{\gamma}$
Experimental				26.3 ± 3.2 [a]				1448 ± 50 [a]
SCF	aug-cc-pVDZ	31.80	5.78	26.02	1022.9	582.4	282.5	741.2
	aug-cc-pVTZ	31.88	5.61	25.86	1081.4	731.4	310.2	854.6
	aug-cc-pVQZ	31.53	5.13	25.08	1146.8	826.5	335.5	938.6
	aug-cc-pV5Z	31.50	5.00	24.90	1169.5	878.8	347.7	980.7
	d-aug-cc-pVDZ	31.70	4.88	24.87	1222.2	843.4	353.9	977.3
	d-aug-cc-pVTZ	31.42	5.14	25.01	1187.0	897.3	357.6	1002.1
	d-aug-cc-pVQZ	31.43	4.96	24.80	1190.3	909.0	358.7	1009.9
MP2	aug-cc-pVDZ	30.28	8.56	28.44	1488.2	877.9	405.7	1090.4
	aug-cc-pVTZ	29.44	8.10	27.39	1517.1	1052.2	429.3	1208.0
	aug-cc-pVQZ	29.00	7.55	26.46	1591.4	1175.1	461.1	1313.8
	aug-cc-pV5Z	28.94	7.39	26.23	1612.1	1238.7	476.0	1363.9
	d-aug-cc-pVDZ	30.18	7.67	27.31	1792.0	1261.9	507.8	1437.6
	d-aug-cc-pVTZ	28.97	7.61	26.52	1669.8	1284.2	495.9	1415.6
	d-aug-cc-pVQZ	28.95	7.37	26.22	1656.4	1292.2	494.5	1416.1
MP3	aug-cc-pVDZ	30.31	8.00	27.79	1325.3	794.1	361.9	978.1
	aug-cc-pVTZ	29.48	7.31	26.46	1340.1	940.6	381.2	1074.7
	aug-cc-pVQZ	29.00	6.73	25.47	1397.7	1040.8	405.1	1158.7
	aug-cc-pV5Z	28.90	6.54	25.19	1413.7	1095.2	417.0	1200.4
	d-aug-cc-pVDZ	30.29	7.12	26.71	1598.9	1138.6	455.1	1291.1
	d-aug-cc-pVTZ	28.95	6.82	25.55	1467.1	1141.4	437.7	1252.3
	d-aug-cc-pVQZ	28.89	6.54	25.18	1447.8	1136.0	431.8	1240.8
MP4	aug-cc-pVDZ	29.01	9.10	28.33	1574.3	922.1	415.7	1139.2
	aug-cc-pVTZ	28.21	8.56	27.19	1587.8	1086.0	437.4	1246.7
	aug-cc-pVQZ	27.90	8.05	26.40	1652.9	1202.0	465.9	1344.4
	aug-cc-pV5Z	27.90	7.90	26.22	1671.8	1263.0	480.2	1392.1
	d-aug-cc-pVDZ	29.13	8.37	27.52	1893.6	1307.4	519.5	1491.6
	d-aug-cc-pVTZ	27.79	8.12	26.41	1741.8	1313.5	503.0	1451.3
	d-aug-cc-pVQZ	27.85	7.88	26.17	1716.0	1311.5	497.7	1440.8
CCSD	aug-cc-pVDZ	30.59	8.80	28.91	1500.5	888.4	402.5	1095.9
	aug-cc-pVTZ	29.56	7.98	27.31	1476.5	1016.4	411.5	1166.6
	aug-cc-pVQZ	29.15	7.41	26.38	1526.1	1116.5	433.9	1247.8
	aug-cc-pV5Z	29.08	7.24	26.14	1540.6	1171.1	445.9	1289.4
	d-aug-cc-pVDZ	30.56	7.97	27.91	1795.8	1255.3	499.5	1428.3
	d-aug-cc-pVTZ	29.05	7.52	26.45	1612.5	1227.0	470.9	1353.6
	d-aug-cc-pVQZ	29.06	7.24	26.12	1580.7	1215.8	462.2	1334.4
CCSD(T)	aug-cc-pVDZ	30.70	9.28	29.56	1618.5	962.0	430.5	1181.2
	aug-cc-pVTZ	29.27	8.48	27.74	1601.0	1104.2	441.5	1262.3
	aug-cc-pVQZ	28.79	7.91	26.77	1654.5	1213.2	465.5	1350.3
	aug-cc-pV5Z	28.70	7.74	26.51	1669.6	1271.9	478.2	1394.8

Table 7 Continued

Method	Basis set	β_{zzz}	β_{xxz}	$\bar{\beta}$	γ_{zzzz}	γ_{xxxx}	γ_{zzxx}	$\bar{\gamma}$
	d-aug-cc-pVDZ	30.60	8.49	28.54	1940.2	1361.1	534.2	1541.3
	d-aug-cc-pVTZ	28.75	8.01	26.86	1748.6	1333.2	505.2	1464.9
	d-aug-cc-pVQZ	28.71	7.73	26.50	1714.1	1321.7	496.0	1444.6

[a] Ground vibrational state, dynamic value referenced by Shelton and Rice [74] with SCF dispersion of Sekino and Bartlett [75].

than 1.4 a.u. Hence, nondynamical correlation is much more important for the first hyperpolarizability than for the dipole polarizability.

With the inclusion of dynamical correlation, the isotropic first hyperpolarizability increases by about 7% (CCSD(T) compared with SCF with the d-aug-cc-pVQZ basis set). However, the effect on the individual components is actually larger; both β_{zzz} and β_{zxx} change by about 2.7 a.u. As with the SCF values, multiple diffuse functions significantly increase the convergence rate of this property, especially for the β_{zxx} component. As shown in Tables 7 and 8 and especially Fig. 11, both the aug-cc-pVnZ and d-aug-cc-pVnZ basis set results converge smoothly from above. The regular convergence of the d-aug series of basis sets allows a reliable estimation of the basis

Table 8
Calculated first and second hyperpolarizabilities (in a.u.) of CO compared with experiment (at $r=2.1322a_0$). Methods based on a multiconfigurational wave function

Method	Basis set	β_{zzz}	β_{xxz}	$\bar{\beta}$	γ_{zzzz}	γ_{xxxx}	γ_{zzxx}	$\bar{\gamma}$
Experimental [a]				26.3 ± 3.2				1448 ± 50
CASSCF	aug-cc-pVDZ	30.09	7.19	26.68	1118.9	701.0	319.7	853.4
	aug-cc-pVTZ	30.16	7.06	26.58	1177.3	864.8	347.7	974.9
	aug-cc-pVQZ	30.00	6.70	26.04	1245.9	965.3	374.0	1063.2
	aug-cc-pV5Z	30.03	6.60	25.94	1267.7	1018.5	386.7	1106.1
	d-aug-cc-pVDZ	30.36	6.57	26.10	1335.3	988.1	394.3	1109.5
	d-aug-cc-pVTZ	29.91	6.75	26.05	1286.5	1035.9	395.6	1126.3
	d-aug-cc-pVQZ	29.97	6.58	25.88	1289.8	1047.1	397.1	1134.1
CAS-CI	aug-cc-pVDZ	30.61	8.77	28.89	1456.8	881.1	393.2	1075.8
	aug-cc-pVTZ	29.51	7.93	27.22	1420.8	1005.0	399.9	1140.0
	aug-cc-pVQZ	29.10	7.38	26.31	1465.9	1097.5	420.7	1215.0
	aug-cc-pV5Z	29.04	7.21	26.07	1478.3	1149.2	431.8	1254.0
	d-aug-cc-pVDZ	30.64	8.05	28.04	1741.5	1241.3	486.3	1399.4
	d-aug-cc-pVTZ	29.08	7.53	26.48	1550.0	1206.2	456.5	1318.5
	d-aug-cc-pVQZ	29.04	7.23	26.10	1517.5	1192.7	447.0	1297.2
CAS-CI + Q	aug-cc-pVDZ	30.61	9.29	29.52	1608.8	962.9	425.7	1175.8
	aug-cc-pVTZ	29.40	8.43	27.75	1577.8	1095.5	437.0	1249.5
	aug-cc-pVQZ	28.98	7.85	26.81	1616.9	1189.4	456.5	1322.9
	aug-cc-pV5Z	28.93	7.68	26.58	1630.6	1249.2	465.4	1364.7
	d-aug-cc-pVDZ	30.54	8.51	28.53	1934.0	1356.5	530.7	1534.9
	d-aug-cc-pVTZ	28.91	7.98	26.92	1705.7	1300.2	490.1	1426.6
	d-aug-cc-pVQZ	28.91	7.69	26.57	1667.8	1287.4	480.3	1404.4

[a] See the footnote to Table 7.

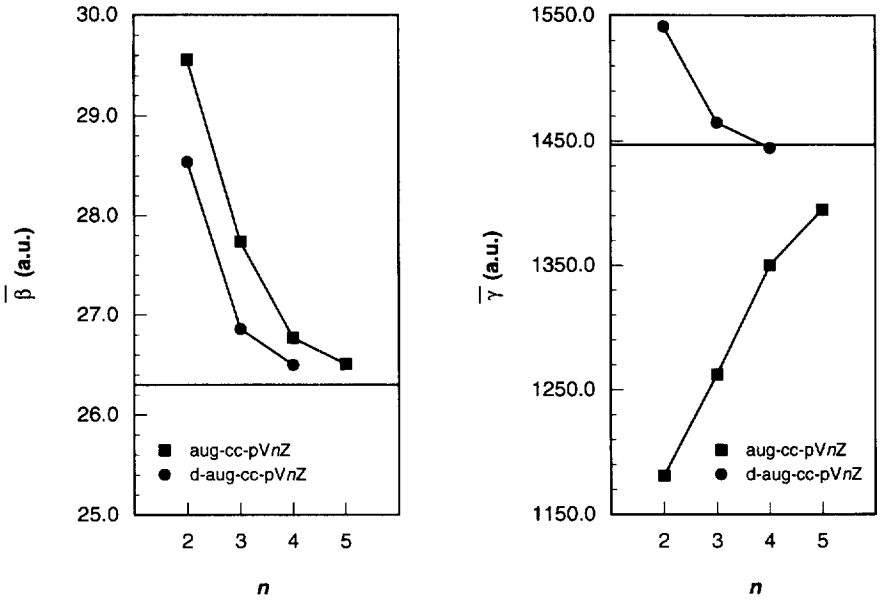

Fig. 11. Calculated CCSD (T) values of the equilibrium first (β) and second (γ) hyperpolarizabilities as a function of the aug-cc-pVnZ and d-aug-cc-pVnZ basis sets. The horizontal solid lines are the experimental values. See the text.

set limit by fitting to the standard exponential function. At the CCSD(T) level, the CBS limit for $\bar{\beta}$ is estimated to be 26.4 a.u., which is only 0.1 a.u. smaller than the d-aug-cc-pVQZ result and arises predominately from a slight decrease in the β_{zxx} component. Our CCSD(T) results for β are in excellent agreement with those from the recent work of Maroulis, as well as with the experimental value shown in Tables 7 and 8. The CCSD(T) values of β_{zzz} (30.17 a.u.) by Kobayashi et al. [76] and $\bar{\beta}$ (23.5 a.u.) by Sekino and Bartlett [75] are somewhat too large and too small, respectively, compared with the estimated limits from the present work. For the other correlation methods shown in Tables 7 and 8, the effect of triples in the CCSD(T) calculations is relatively small, only 0.4 a.u. in the isotropic value. The MPn methods also yield good results for the first dipole hyperpolarizability. In general, they result in values of $\bar{\beta}$ slightly lower than those of CCSD(T). For the individual components, however, MP2 yields a β_{zzz} in better agreement with CCSD(T) than MP4, which is lower by nearly 1 a.u. with the d-aug-cc-pVQZ basis set. For the multireference methods, both CAS + 1 + 2 and CAS + 1 + 2 + Q yield accurate values for β with the latter agreeing most closely with CCSD(T).

For the SCF values of the 2nd hyperpolarizabilities γ, excellent convergence with respect to extensions of the basis set is also observed, especially for the d-aug-cc-pVnZ basis sets. The HF limits are estimated from the d-aug-cc-pVQZ results to be $\gamma_{zzzz} = 1190$ a.u., $\gamma_{xxxx} = 910$ a.u., $\gamma_{xxzz} = 360$ a.u., and $\bar{\gamma}$ = 1010 a.u. All of these values are very similar to those of Maroulis [64], as well as those of Sekino and Bartlett [75]. Nondynamical correlation, as indicated by the difference between SCF and CASSCF, increases all three components of γ by 8–15% with the d-aug-cc-pVQZ basis set. The resulting effect on $\bar{\gamma}$ is +12% or 124 a.u. As expected, dynamical correlation has a large effect on the computed 2nd hyperpolarizabilities, increasing all components relative to the SCF values by about 40%. In this case MP4 is in very good agreement with the CCSD(T) values, while the CAS + 1 + 2 or CAS + 1 + 2 + Q results are somewhat too low. In Fig. 11, the convergence behavior of the CCSD(T) values of $\bar{\gamma}$ are observed to be very regular with the aug-cc-pVnZ values converging from above and the d-aug-cc-pVnZ results converging from below. Extrapolation of the d-aug values yields an estimate for the CCSD(T)/CBS limit of 1435 a.u. for the static $\bar{\gamma}$, which is only slightly smaller than our directly calculated d-aug-cc-pVQZ result and in excellent

agreement with the estimated static experimental value. Our results suggest that the CCSD(T) values recently obtained by Maroulis for $\bar{\gamma}$ and the components of γ are slightly too large, while those obtained by Sekino and Bartlett, where a much more modest basis set was used, are too large by about 10%. In addition, the CCSD(T) results of Kobayashi et al. for γ_{zzzz} are larger than our d-aug-cc-pVQZ result by 5%, however their value of γ_{xxxx} is nearly identical to our result.

4. Conclusions

The accuracy of molecular electronic wave functions is determined by two expansions: the many-electron expansion in terms of molecular orbitals that defines the form of the wave function and the basis set used to expand the one-electron molecular orbitals. By carefully controlling the errors in the calculations, it is possible to compute the properties of small molecules to an accuracy that rivals that available from all but the most sophisticated experimental studies. Central to this is the ability to quantify the intrinsic errors of the electron correlation methods in common use today: multireference (icCAS + 1 + 2), perturbation theory (MP2, MP3, MP4), and coupled cluster [CCSD, CCSD(T)] techniques.

With the recently developed correlation consistent basis sets it is possible to systematically converge most molecular properties to the complete basis set limit. Considering first the valence electron calculations, we find the icCAS + 1 + 2 (including + Q) and CCSD(T) methods to provide uniformly high accuracy—predicting D_e to within 1.0 kcal mol^{-1}, r_e to within 0.002 Å, ω_e to within 4 cm^{-1}, and μ_e to within 0.04 D of the measured values. Surprisingly, the converged perturbation theory calculations often lead to MP4 results that are decidedly less accurate than the corresponding MP2 results, e.g., for r_e the errors are 0.0056 Å (MP2) and 0.0125 Å (MP4) and for ω_e the errors are -42 cm^{-1} (MP2) and -147 cm^{-1} (MP4). This suggests that the Møller–Plesset perturbation expansion may not be convergent for some molecular properties, at least for low orders of perturbation theory. It certainly establishes that use of higher orders of perturbation theory does not guarantee higher accuracy.

Inclusion of core/core–valence correlation effects can substantially reduce the errors in the calculated spectroscopic constants. For example, for the CCSD(T) method the errors in the all-electron calculation are just –0.1 kcal mol^{-1} (D_e), 0.0004 Å (r_e), and 6 cm^{-1} (ω_e); the reason for the increase in the error for ω_e is not well understood at this point. It could very well be due, however, to slight inadequacies in the correlation treatment since all-electron CAS + 1 + 2 + Q has an intrinsic error of just 2 cm^{-1}.

With the addition of shells of diffuse functions to the cc-pV*n*Z basis sets, either aug-cc-pV*n*Z or d-aug-cc-pV*n*Z, it is also possible to systematically converge molecular electric properties such as dipole moments and even hyperpolarizabilities.

Acknowledgements

This work was supported by the Division of Chemical Sciences in the Office of Basic Energy Sciences of the U.S. Department of Energy. The Pacific Northwest National Laboratory is a multiprogram national laboratory operated for the Department of Energy by Battelle Memorial Institute, under Contract No. DE-AC06-76RLO 1830. Computational resources for this work were provided by the Division of Chemical Sciences and by the Division of Mathematics, Information, and Computational Sciences, Office of Computational and Technology Research, at the National Energy Research Supercomputing Center (Livermore, California). The authors wish to thank Dr R.A. Kendall for prepublication review of the manuscript.

References

[1] T.H. Dunning, Jr., J. Chem. Phys. 90 (1989) 1007.
[2] R.A. Kendall, T.H. Dunning, Jr., R.J. Harrison, J. Chem. Phys. 96 (1992) 6796.
[3] D.E. Woon, T.H. Dunning, Jr., J. Chem. Phys. 98 (1993) 1358.
[4] D.E. Woon, T.H. Dunning, Jr., J. Chem. Phys. 100 (1994) 2975.
[5] D.E. Woon, T.H. Dunning, Jr., J. Chem. Phys. 103 (1995) 4572.
[6] A.K. Wilson, T. van Mourik, T.H. Dunning, Jr., J. Mol. Struct., 388 (1996) 339.
[7] D.E. Woon, T.H. Dunning, Jr., J. Chem. Phys. 99 (1993) 1914.
[8] K.A. Peterson, R.A. Kendall, T.H. Dunning, Jr., J. Chem. Phys. 99 (1993) 1930.

[9] K.A. Peterson, R.A. Kendall, T.H. Dunning, Jr., J. Chem. Phys. 99 (1993) 9790.
[10] K.A. Peterson, D.E. Woon, T.H. Dunning, Jr., J. Chem. Phys. 100 (1994) 7410.
[11] D.E. Woon, J. Chem. Phys. 100 (1994) 2838.
[12] D.E. Woon, T.H. Dunning, Jr., J. Chem. Phys. 101 (1994) 8877.
[13] K.A. Peterson, T.H. Dunning, Jr., J. Chem. Phys. 102 (1995) 2032.
[14] K.A. Peterson, J. Chem. Phys. 102 (1995) 262.
[15] K.A. Peterson, T.H. Dunning, Jr., J. Phys. Chem. 99 (1995) 3898.
[16] K.A. Peterson, D.E. Woon, A.K. Wilson, T.H. Dunning, Jr., Theor. Chem. Acc., in press.
[17] A.K. Wilson, T.H. Dunning, Jr., J. Chem. Phys. 106 (1997) 8718.
[18] C. Møller, M.S. Plesset, Phys. Rev. 46 (1934) 618.
[19] C. Hampel, K.A. Peterson, H.-J. Werner, Chem. Phys. Lett. 190 (1992) 1.
[20] H.-J. Werner, P.J. Knowles, J. Chem. Phys. 82 (1985) 5053.
[21] P.J. Knowles, H.-J. Werner, Chem. Phys. Lett. 115 (1985) 259.
[22] K. Stark, H.-J. Werner, J. Chem. Phys. 104 (1996) 6515.
[23] H-J. Werner, P.J. Knowles, J. Chem. Phys. 89 (1988) 5803.
[24] P.J. Knowles, H.-J. Werner, Chem. Phys. Lett. 145 (1988) 514.
[25] S.R. Langhoff, E.R. Davidson, Int. J. Quantum Chem. 8 (1974) 61.
[26] M.R.A. Blomberg, P.E.M. Siegbahn, J. Chem. Phys. 78 (1983) 5682.
[27] J. Simons, J. Phys. Chem. 93 (1989) 626.
[28] C.W. Bauschlicher, Jr., H. Partridge, J. Chem. Phys. 100 (1994) 4329.
[29] H. Partridge, C.W. Bauschlicher, Jr., J. Chem. Phys. 103 (1995) 10589.
[30] A.G. Császár, W.D. Allen, J. Chem. Phys. 104 (1996) 2746.
[31] K.A. Peterson, T.H. Dunning, Jr., J. Chem. Phys., 106 (1997) 4119.
[32] R.J. Gdanitz, R. Ahlrichs, Chem. Phys. Lett. 143 (1988) 413.
[33] H.-J. Werner, P.J. Knowles, Theor. Chim. Acta 78 (1990) 175.
[34] J.L. Dunham, Phys. Rev. 41 (1932) 721.
[35] W.J. Lauderdale, J.F. Stanton, J. Gauss, J.D. Watts, R.J. Bartlett, Chem. Phys. Lett. 187 (1991) 21.
[37] P.J. Knowles, C. Hampel, H.-L Werner, J. Chem. Phys. 99 (1994) 5219.
[38] M.J.O. Deegan, P.J. Knowles, Chem. Phys. Lett. 227 (1994) 321.
[40] C.E. Moore, Atomic Energy Levels, NSRDS-NBS 35, Office of Standard Reference Data, National Bureau of Standards, Washington, DC, 1971.
[41] A.E. Douglas, C.K. Moller, Can.J. Phys. 33 (1955) 125.
[42] K.P. Huber, G. Herzberg, Molecular Spectra and Molecular Structure, IV. Constants of Diatomic Molecules, Van Nostrand, Princeton, NJ, 1979.
[43] M.W. Chase, Jr., C.A. Davies, J.R. Downey, Jr., D.J. Frurip, R.A. McDonald, A.N. Syverud, J. Phys. Chem. Ref. Data 14, Suppl. No. 1 (1985).
[44] S.R. Langhoff, C.W. Bauschlicher, Jr., J. Chem. Phys. 102 (1995) 5220.
[45] M. Ernzerhof, C.M. Marian, S.D. Peyerimhoff, Chem. Phys. Lett. 204 (1993) 59.
[46] R.J. Bartlett, G.D.I. Purvis, Phys. Rev. A 20 (1979) 1313.
[47] S.M. Kirschner, J.K.G. Watson, J. Mol. Spectrosc. 47 (1973) 234).
[48] J.W. Cooley, Math. Comput. 15 (1961) 363.
[49] J.S. Muenter, J. Mol. Spectrosc. 55 (1975) 490.
[50] W.L. Meerts, F.H. De Leeuw, A. Dymanus, Chem. Phys. 22 (1977) 319.
[51] D. Sundholm, P. Pyykkö, L. Laaksonen, Mol. Phys. 56 (1985) 1411.
[52] K.A. Peterson, T.H. Dunning, Jr., in preparation.
[53] B. Rosenblum, A.H. Nethercot, C.H. Townes, Phys. Rev. 109 (1958) 400.
[54] R.K. Nesbet, J. Chem. Phys. 40 (1964) 3619.
[55] W.M. Huo, J. Chem. Phys. 43 (1965) 624.
[56] C.A. Burrus, J. Chem. Phys. 28 (1958) 427.
[57] I. Ozier, P. Yi, A. Kohosla, N.F. Ramsey, J. Chem. Phys. 46 (1967) 1530.
[58] I. Ozier, L.M. Crapo, N.F. Ramsey, J. Chem. Phys. 49 (1968) 2314.
[59] F.P. Billingsley, M. Krauss, J. Chem. Phys. 60 (1974) 4130.
[60] D. Feller, C.M. Boyle, E.R. Davidson, J. Chem. Phys. 86 (1987) 3424.
[61] G.E. Scuseria, M.D. Miller, F. Jensen, J. Geertsen, J. Chem. Phys. 94 (1991) 6660.
[62] P. Botschwina, M. Horn, J. Flügge, S. Seeger, J. Chem. Soc. Faraday Trans. 89 (1993) 2219.
[63] J.M. Luis, J. Martí, M. Duran, J.L. Andrés, J. Chem. Phys. 102 (1995) 7573.
[64] G. Maroulis, J. Phys. Chem. 100 (1996) 13466.
[65] H.-J. Werner, Mol. Phys. 44 (1981) 111.
[66] D.L. Cooper, K. Kirby, J. Chem. Phys. 87 (1987) 424.
[67] E.R. Cohen, B.N. Taylor, Rev. Mod. Phys. 59 (1987) 1121.
[68] C. Chackerian, Jr., R.H. Tipping, J. Mol. Spectrose. 99 (1983) 431.
[69] G.A. Parker, R.T. Pack, J. Chem. Phys. 64 (1976) 2010.
[70] N.J. Bridge, A.D. Buckingham, Proc. R. Soc. London, Ser. A 295 (1966) 334.
[71] F. Baas, K.D. Van den Hout, Physica 95A (1979) 597.
[72] C. Asawaroengchai, G.M. Rosenblatt, J. Chem. Phys. 72 (1980) 2664.
[73] H. Kling, W. Hüttner, Chem. Phys. 90 (1984) 207.
[74] D.P. Shelton, J.E. Rice, Chem. Rev. 94 (1994) 3.
[75] H. Sekino, R.J. Bartlett, J. Chem. Phys. 98 (1993) 3022.
[76] R. Kobayashi, H. Koch, P. Jørgensen, T.J. Lee, Chem. Phys. Lett. 211 (1993) 94.